Molecular Phylogenetics and Evolution 219 (2026) 108551

Contents lists available at ScienceDirect

Molecular Phylogenetics and Evolution

journal homepage: www.elsevier.com/locate/ympev

The legacy of the paleotropical flora belt: extreme continental vicariance and island refugia in Woodwardioid ferns

Guillermo Santos [a,*], Mario Fernández-Mazuecos [b,c,d,*], Cornelia Krause [e], Sonia Molino [a,f,g], Anita Roth-Nebelsick [e], Mike Thiv [e,1,*], Mario Mairal [a,1,*]

[a] Department of Biodiversity, Ecology and Evolution, Universidad Complutense de Madrid, Calle de José Antonio Novais 12, 28040 Madrid, Spain
[b] Department of Biodiversity and Conservation, Real Jardín Botánico (RJB), CSIC, Plaza de Murillo 2, 28014 Madrid, Spain
[c] Centro de Investigación en Biodiversidad y Cambio Global (CIBC-UAM), Universidad Autónoma de Madrid, Calle Darwin 2, 28049 Madrid, Spain
[d] Department of Biology (Botany), Faculty of Science, Universidad Autónoma de Madrid, Calle Darwin 2, 28049 Madrid, Spain
[e] State Museum of Natural History, 70191, Stuttgart, Germany
[f] Department of Biosciences, Faculty of Biomedical and Health Sciences, Universidad Europea de Madrid, 28670 Madrid, Spain
[g] Instituto de Investigación en Cambio Global-Universidad Rey Juan Carlos, Móstoles, 28933 Madrid, Spain

ARTICLE INFO

Keywords:
Climatic corridors
Intracontinental disjunction
Paleotropical flora
Subtropical refugia
Vicariance-driven speciation
Back-colonization
Woodwardia radicans
Woodwardioideae

ABSTRACT

The distribution of vegetation across the Northern Hemisphere has been profoundly shaped by the climatic and geological history of the Cenozoic. An ancient paleotropical vegetation belt, once spanning the Northern Hemisphere, is hypothesized to have facilitated biotic exchange across regions during the early Cenozoic, before its eventual fragmentation and near-complete disappearance. We investigate the evolutionary history of this pattern using the fern subfamily Woodwardioideae (Blechnaceae)—a striking example of disjunction across the Northern Hemisphere. By integrating phylogenetic relationships, divergence times and ancestral range dynamics based on plastid and genome-wide genotyping-by-sequencing markers, complemented by a review of the fossil record, ecological niche modelling and paleoclimate simulations, we reconstruct the spatio–temporal colonization history of this group. Our results suggest a vicariance-driven speciation process facilitated by climatic change. Notably, we identify intracontinental vicariance between the sister species *Woodwardia radicans* and *W. unigemmata* across Eurasia in the Pliocene, likely driven by the extinction of intermediate populations, which confined these species to opposite ends of Eurasia, corresponding to late-Cenozoic refugia of the paleotropical (lauroid) element. Extinction in the Western Palearctic appears to have been more severe than in the East, leading continental populations of *W. radicans* to retreat to the Macaronesian archipelagos, from which they back-colonized small continental and Mediterranean island enclaves in the Pleistocene. These findings underscore the role of islands as both crucial reservoirs for paleotropical-affinity relicts and sources of diversity for adjacent continental enclaves. They also emphasize both island and continental refugia as the last reservoirs of the evolutionary legacy of paleotropical-affinity lineages, and highlight their vulnerability to ongoing climate change.

1. Introduction

The distribution of plant biodiversity on Earth has fluctuated throughout history, shaped by changing climates and geological events. Factors such as long-distance dispersal, migration through biotic corridors, and extinction have played pivotal roles in forming the distribution patterns we observe today (Mai, 1991; Muñoz et al., 2004; Mairal et al., 2015; Graham, 2018; De Kort et al., 2021). Understanding the temporal dynamics of floristic elements—how vegetation has responded to climate changes across various spatial and temporal scales—offers essential insights into the processes that have shaped ecosystems, which is especially relevant in the context of the ongoing climate change crisis (McLaughlin, 1994; McElwain, 2018; Aguado-Lara et al., 2025). In this way, examining vegetation dynamics from the early Cenozoic era to the

* Corresponding authors.
E-mail addresses: gsanto02@ucm.es, santosrivilla24@gmail.com (G. Santos), mfmazuecos@rjb.csic.es (M. Fernández-Mazuecos), mike.thiv@smns-bw.de (M. Thiv), mariomai@ucm.es (M. Mairal).
[1] Contributed equally as senior authors.

https://doi.org/10.1016/j.ympev.2026.108551
Received 19 July 2025; Received in revised form 14 January 2026; Accepted 17 January 2026
Available online 22 January 2026

present offers a valuable lens for understanding the interplay between geological and climatic events in shaping biodiversity over recent geological epochs (Zachos et al., 2008; Barrón et al., 2010).

To understand the current patterns of floristic diversity, it may be useful to trace their origins back to the onset of the Cenozoic. This era began following a major extinction event that drastically reduced both animal and plant life (Alvarez et al., 1980; Nichols and Johnson, 2008; Uriarte Cantolla, 2003). The early Cenozoic was marked by high temperatures and monsoonal rains in southern Europe and northern Africa, driven by a warm seawater current flowing through the Tethys Sea (Torfstein and Steinberg, 2020; Uriarte Cantolla, 2003). During this time, significant climatic and orogenic changes profoundly impacted biodiversity (Tiffney and Manchester, 2001). Key geological events such as the Alpine and Himalayan orogeny reshaped European and Asian landscapes, creating significant geographical barriers that influenced species migration and isolation (Tiffney and Manchester, 2001). Concurrently, global cooling during the Eocene-Oligocene transition drastically reduced tropical habitats, leading to the expansion of temperate ecosystems (Collinson, 1992; Wolfe, 1992). These climatic and geological dynamics resulted in the formation of trans-oceanic latitudinal vegetation belts (Chaney, 1959; Axelrod, 1958, 1975; Wolfe, 1981; Mai, 1991; Barrón, 2003). Across the Northern Hemisphere, these vegetation belts included two major floristic elements: the arctotertiary element, characterized by coniferous and mixed deciduous forests, dominated higher latitudes, while the paleotropical element, characterized by broadleaf evergreen and laurel forests, occupied mid- to low-latitudes (also known as “boreotropical”; Engler, 1882; Mai, 1989, 1991). As the Cenozoic progressed, the closure of the Tethys Sea (Hamon et al., 2013), along with the Himalayan uplift (Raymo et al., 1988), contributed to a gradual cooling trend, followed by the Late Miocene Cooling (ca. 11.6–5.3 Ma; Herbert et al., 2016). This cooling favored the expansion of the arctotertiary element into cooler climates and more southerly latitudes (Walther, 1994; Barrón et al., 2010). As a result, the paleotropical element began to retreat, with its former continuity progressively replaced by fragmented, refugial distributions of paleotropical-affinity (lauroid) taxa, a process further accelerated in subsequent stages, including events such as the Messinian Salinity Crisis (Krijgsman et al., 1999) and Plio-Pleistocene glaciations (Hewitt, 1999; Schmitt, 2007). These combined factors created increasingly challenging conditions for the paleotropical element in the Northern Hemisphere (Milne and Abbott, 2002; Mai, 1989; Kovar-Eder et al., 2006), leading to the extinction of numerous taxa by the late Pliocene (Postigo-Mijarra et al., 2009), while allowing some species to persist in climatically favorable regions, such as the southern continental margins of North America and Asia (Chen and Lou, 2019; Stewart et al., 2010). In contrast, western Eurasia faced higher extinction rates due to major geographic and climatic barriers (Mairal et al., 2017; Milne and Abbott, 2002; Tiffney, 1985), which likely resulted in fewer surviving lineages. In this context, intra-continental disjunctions within Europe are thought to arise from the combined effects of these historical climatic oscillations, repeated range contractions, and the fragmentation of formerly continuous vegetation belts. Such processes led to the establishment of multiple refugial areas—particularly in the Iberian, Italian and Balkan peninsulas—where relict lineages persisted through adverse climatic phases (Hewitt, 2000; Médail and Diadema, 2009). Studying these disjunctions is therefore crucial for understanding how extinction, survival in refugia and post-glacial recolonization have shaped present-day European plant diversity, as well as for identifying the evolutionary and biogeographical mechanisms underlying these relict distributions. In this sense, intracontinental vicariance in western Eurasia appears less well documented than the well-known disjunctions between eastern Asia and eastern North America (Wen et al., 2016). Despite this, current evidence shows that some lineages persisted in refugia within the Mediterranean Basin and in more peripheral regions, such as the Macaronesian archipelagos (Benítez-Benítez et al., 2018; Fernández-Palacios et al., 2011; Mairal et al., 2015, 2017; Valcárcel et al., 2017; Vitelli et al., 2017). Mediterranean peninsulas and islands, as well as the Macaronesian archipelagos, acted as glacial refugia during the Pleistocene for some subtropical lineages that were previously widespread (García-Verdugo et al., 2021; Hewitt, 2011; Mairal et al., 2015, 2018; Médail and Diadema, 2009; Nieto Feliner, 2014). These refugia played a critical role in preserving biodiversity, leaving a visible imprint on the distribution and phylogeographic patterns of various lineages that persisted in Pleistocene refugia (Guerra Montes, 2018; Krause et al., 2022; Migliore et al., 2012; Zachos et al., 2008). Despite these insights, it is still debated whether populations of paleotropical-affinity species in these refugia have remained stable for millions of years throughout the Cenozoic or were instead established more recently during the Pliocene/Pleistocene (Calleja et al., 2009; Kondraskov et al., 2015).

The study of paleotropical-affinity lineages confined to these refugia would provide valuable insights into the spatiotemporal evolution of the paleotropical element throughout the Northern Hemisphere. A prime example within this element is the fern flora, which comprises a set of lineages that were dominant in the undergrowth of these paleotropical forests (Barrón et al., 2010; Fernández-Palacios et al., 2011; Schuler et al., 2021). Ferns such as *Culcita macrocarpa* C.Presl, *Davallia canariensis* (L.) Sm., *Diplazium caudatum* (Cav.) Jermy, *Hymenophyllum tunbrigense* (L.) Sm., *Stegnogramma pozoi* (Lag.) K.Iwats., and *Vandenboschia speciosa* (Willd.) G.Kunkel are recognized as representative elements of the paleotropical (palaeo)flora. These ferns were likely widespread in the past but are now restricted to scattered climatic refugia across the Northern Hemisphere (Fernández-Palacios et al., 2011). Among the most widespread and emblematic fern lineages associated with lauroid vegetation across the Northern Hemisphere is the genus *Woodwardia* Sm., belonging to the family Blechnaceae within the subfamily Woodwardioideae (Gasper et al., 2017; PPG I, 2016). This subfamily comprises three genera, two of which are monotypic (*Anchistea* C.Presl and *Lorinseria* C.Presl), while *Woodwardia* includes 13 species (Gasper et al., 2017). *Woodwardia* species are found in temperate and subtropical zones of the Northern Hemisphere: four species are endemic to North and Central America, and the remaining species are endemic to Eurasia, with some isolated occurrences on islands of Oceania (Cranfill and Kato, 2003). This distribution includes a remarkable intracontinental disjunction across the Northern Hemisphere, separating the two sister species *Woodwardia radicans* (L.) Sm. and *W. unigemmata* (Makino) Nakai (Cranfill and Kato, 2003; Gasper et al., 2017), with an extensive range spanning over 5,000 km, making it one of the largest known intracontinental disjunctions (Fig. 1). *Woodwardia radicans*, commonly known as the chain fern or “píjara”, inhabits the western side of the disjunction, including the Macaronesian archipelagos (Azores, Madeira and Canary Islands) and small isolated patches across the Western Palearctic. These include scattered localities in the northwestern Iberian Peninsula and the Mediterranean Basin (Algeria, Italy, Corsica, Sicily, Crete; Fig. 1). This distribution reflects areas of Atlantic influence, where tropical and paleomediterranean elements predominate (Salvo Tierra, 1990; Fernández-Palacios et al., 2011)—humid habitats that are now highly restricted and significantly threatened by habitat alteration and climate change. In contrast, on the eastern part of the disjunction, *W. unigemmata* exhibits a much broader distribution, ranging from the eastern Himalayas to Japan, with localities in central and southern China and extending into lower latitudes such as the Philippines, Taiwan, and New Guinea (Fig. 1).

Continental-scale disjunct distribution patterns are particularly significant in the context of the current biodiversity crisis, as they are often linked to climate-driven extinctions that fragmented once-continuous biotas (Axelrod and Raven, 1978; Crisp and Cook, 2007; Mairal et al., 2015, 2018). In this context, we hypothesize that the intracontinental disjunction between *W. radicans* and *W. unigemmata* aligns with the extremes of the hypothesized paleotropical vegetation belt that extended across the Northern Hemisphere during the early Cenozoic (Axelrod, 1975; Mai, 1991), potentially representing a post-boreotropical relict of this once-continuous lineage (Pichi-Sermolli,

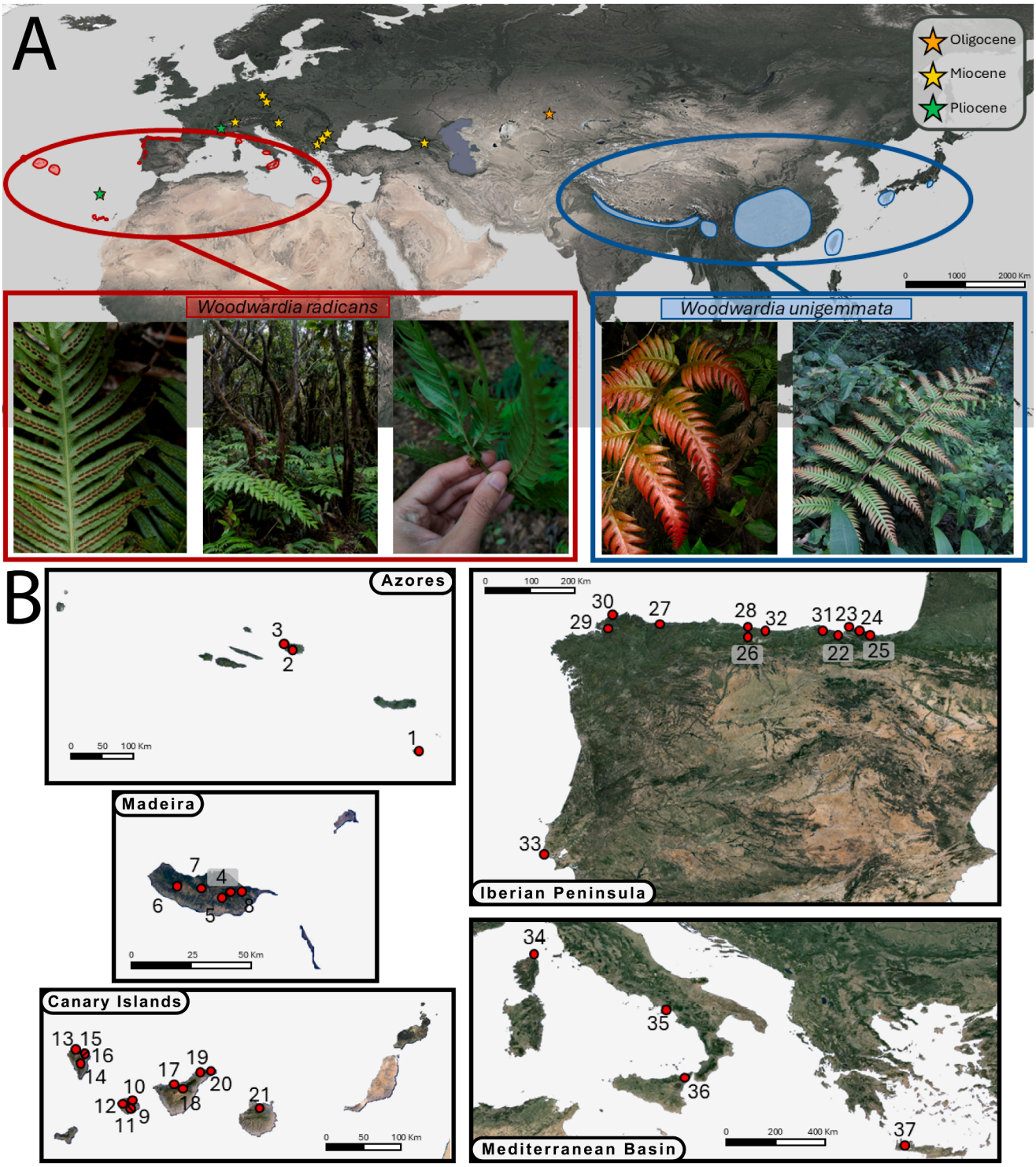

Fig. 1. (A) Disjunct geographic distribution of the sister species *Woodwardia radicans* (red) and *W. unigemmata* (blue) across the Palearctic and their morphology. Photos of *W. unigemmata* by Liang Zhang, and photos of *W. radicans* by Guillermo Santos. Stars indicate *Woodwardia* fossil records: orange for the Oligocene, yellow for the Miocene, and green for the Pliocene. (B) Sampled populations of *W. radicans*, with numbers corresponding to those in Table 1. Maps were modified from Google Earth. (For interpretation of the references to colour in this figure legend, the reader is referred to the web version of this article.)

1979; Quintanilla et al., 2000). As this belt contracted during the Mio-Pliocene, lineages likely became isolated at its eastern and western extremes. If so, we would expect to find deep genetic divergences indicative of long-term survival in climatic refugia—particularly in *W. radicans* populations in the Western Palearctic, where paleotropical extinction was likely more severe (Hewitt, 2000; Médail and Diadema, 2009). Alternatively, the observed disjunction may result from long-distance dispersal rather than historical continuity. At the same time, the detailed study of the phylogeography and population genomics of *W. radicans* in the Western Palearctic offers an opportunity to understand how these threatened climatic refugia have acted as sanctuaries for the species, influencing its present-day genetic diversity and providing essential guidance for future conservation strategies.

To test these hypotheses, the primary aims of this study were to (1)

reconstruct the phylogeny of the Woodwardioideae subfamily using Bayesian inference to clarify evolutionary relationships and divergence patterns; (2) disentangle the extreme intracontinental disjunction between *W. radicans* and *W. unigemmata* using dated phylogenies and environmental niche modeling (ENM) to understand the impact of past climatic changes on species distribution across the Northern Hemisphere; (3) explore the history and ancestral dynamics of restricted paleotropical refugia of *W. radicans* in the Western Palearctic using genome-wide genotyping-by-sequencing (GBS) data and ENM. By integrating phylogenetic reconstruction, Bayesian Island Biogeographic analyses, and ecological modeling, we aimed to determine how past and present climatic conditions have shaped the evolutionary history of the Woodwardioideae, with a particular focus on the *W. radicans–W. unigemmata* lineage. Additionally, by reconstructing historical changes in distribution range of these species and assessing the role of fossils and climatic refugia for *W. radicans* in the Western Palearctic, this study aims to enhance our understanding of the conservation needs of this species and other paleotropical-affinity lineages.

2. Materials and methods

2.1. Sampling, DNA isolation and quantification

Plant tissue samples were collected during several expeditions conducted between 2013 and 2015 in the Western Palearctic region. We collected leaf samples from 37 populations of *W. radicans* (Table 1) covering both the main continental enclaves and the Macaronesian archipelagos. Voucher specimens for populations that were not previously sampled have been deposited in the MA and STU herbaria (Thiers, 2025). The sampled continental enclaves included the northwest of the Iberian Peninsula (11 populations), Corsica (1 population), the Italian Peninsula (1 population), continental Portugal (1 population from an introduced population in Sintra; Carapeto et al., 2020), Sicily (1 population), and Crete (1 population). In the Macaronesian archipelagos, we sampled individuals from the Azores (3 populations), Madeira (5 populations), and the Canary Islands (13 populations). Whenever possible, we collected more than one individual per population ensuring a minimum spatial distance to avoid clonal sampling. Plant tissue was dried in silica gel. Additionally, we sampled leaf tissue from herbaria (HAST, TNS) or botanical garden specimens of four other *Woodwardia* species, including one of *W. japonica* (L.f.) Sm., one of *W. orientalis* Sw., two of *W. prolifera* Hook. & Arn. and two of *W. unigemmata* (Table 1).

DNA extractions were conducted using 2–3 dried pinnae from each sampled individual. Leaves were crushed using metal beads in a Retsch MM400 mixer mill for 5–10 min at 30 Hz, until a fine powder was obtained. DNA extraction was carried out with the commercial NucleoSpin Plant II Mini Kit (Macherey and Nagel). Quality check was performed on a 0.7% agarose gel by loading 1 μl of the DNA extract and running it for 30 min at 100 V. The concentrations of the extracted DNA were quantified using a spectrophotometer (Implen NanoPhotometer® N60).

Table 1
Sampled populations of *Woodwardia*. Population numbers as in Fig. 1. One individual was sampled per population.

Taxon	Region	Population number	Population	Latitude	Longitude
W. radicans	Azores	1	Cu de Judas	37.0129	−25.0030
		2	Santa Barbara	38.7283	−27.2766
		3	Raminho	38.7650	−27.3183
	Madeira	4	Ribeiro Frio	32.7315	−16.8866
		5	Ribeiro Frio 2	32.7215	−16.9079
		6	Portela	32.7627	−17.1331
		7	Fontes Levada	32.7523	−17.0190
		8	Encumeada	32.7474	−16.8240
	Canary Islands	9	La Gomera – Las Creces	28.1422	−17.1916
		10	La Gomera – Reventón Oscuro	28.1305	−17.2180
		11	La Gomera – Reventón Oscuro 2	28.1156	−17.2192
		12	La Gomera – Mulagua	28.1415	−17.2910
		13	La Palma – Garafía	28.8305	−17.8994
		14	La Palma – Los Tiles	28.6438	−17.8211
		15	La Palma – Los Tiles 2	28.7927	−17.8075
		16	La Palma – Cumbre Nueva	28.7691	−17.7825
		17	Tenerife – Barranco Ruiz	28.3583	−16.5868
		18	Tenerife – Barranco Ruiz 2	28.3677	−16.5997
		19	Tenerife – Chamorga	28.5409	−16.2715
		20	Tenerife – Anaga	28.5648	−16.1673
		21	Gran Canaria – Osorio	28.0741	−15.5464
	Atlantic Iberia	22	Galdames	43.3132	−3.1398
		23	Lemoniz	43.4606	−2.9024
		24	Mundaka	43.4019	−2.6974
		25	Lekeitio	43.3280	−2.4970
		26	Picos de Europa	43.3307	−5.0786
		27	Grilo	43.4925	−6.9783
		28	Purón	43.4250	−5.0804
		29	Fragas do Eume	43.4035	−8.0527
		30	Seixo	43.7127	−7.9510
		31	Carasa	43.3654	−3.4628
		32	Garganta de Urdón	43.4191	−4.7043
	Mainland Portugal	33	Monserrate (introduced)	38.792	−9.4200
	Corsica	34	Dans le Cap	–	–
	Italian Peninsula	35	Amalfi	40.6512	14.5823
	Sicily	36	Scuderi	38.0852	15.3054
	Crete	37	Nea Rumata	35.4005	23.8714
W. unigemmata	China	Wr-Ch1 (botanical garden)	Sangzhi (transplanted to Shanghai Chenshan Botanical Garden)	29.6595	109.1609
	Japan	AE070211-01(herbarium TNS)	Nishizu-cho	–	–
W. prolifera		TBG149712 (botanical garden)	Iriomote (transplanted to Tsukuba Botanical Garden)	–	–
		AE060930-03 (herbarium TNS)	Okinawa	–	–
W. japonica	Taiwan	HAST141012 (herbarium HAST)	Pingtung	22.4183	120.66
W. orientalis	Taiwan	HAST100119 (herbarium HAST)	Pingtung	22.7313	120.7339

These values were used to standardize the samples a posteriori at around 40 ng/μl, which is considered adequate for genotyping-by-sequencing. The 43 genomic DNA samples, adjusted to 40 ng/μl, were organized into 96-well plates.

2.2. Sanger sequencing and phylogenetic inference

To make a preliminary assessment of the phylogenetic relationships and divergence times within the subfamily Woodwardioideae, we retrieved sequences for four plastid DNA (ptDNA) regions—*rps*4, *rbc*L, *atp*B, and *mat*K—from GenBank (National Center for Biotechnology Information, NCBI) and complemented these with newly generated *rps*4 sequences for *W. radicans*, *W. prolifera* and *W. unigemmata* (GenBank accession numbers are listed in Table S1). For the amplification of *rps*4, the standard primers trnS^{GGA} and rps4.5 were used (Small et al., 2005). The reaction mixture consisted of 1 × PCR reaction buffer (containing 2 mM $MgCl_2$), 0.2 mM dNTPs, 0.4 μM each of forward and reverse primer, 0.05 U/μl DreamTaq DNA polymerase (Thermo Fisher Scientific), and 1 μl of the diluted DNA extract as template. PCRs were performed with a Sensoquest or Biometra cycler under the following touchdown conditions: 5 min 94°C, 10 initial cycles (30 s 94°C, 45 s 55°C − 0.5°C/cycle, 90 s 72°C), 25 cycles (30 s 94°C, 45 s 50°C, 90 s 72°C), 10 min 72°C. External Sanger sequencing service was provided by LGC Genomics, Berlin. New sequences were deposited in the GenBank database (NCBI; see Table S1 for accession numbers).

The assembled dataset comprised three outgroup species representing the family Onocleaceae and 31 species representing the family Blechnaceae, with a particular focus on the subfamily Woodwardioideae, encompassing 12 out of 15 representatives following Gasper et al. (2017) (Table S1). Sequences were aligned using the ClustalW v.2.1 algorithm, implemented in Geneious 11.1.5 software (https://www.geneious.com, Kearse et al., 2012; Biomatters Ltd., Auckland, New Zealand). Alignments were then checked manually and adjusted where necessary, following the alignment rules described in Kelchner (2000). To determine the best nucleotide substitution model, we used the Akaike Information Criterion (AIC) value calculated in jModelTest 2.1.10 (Darriba et al., 2012). Subsequently, we concatenated the four ptDNA regions (*rps*4-*rbc*L-*atp*B-*mat*K) into a single matrix. This dataset was used for phylogenetic reconstruction and dating of the Woodwardioideae. Hereafter we refer to this dataset as the "Woodwardioideae ptDNA dataset".

Phylogenetic relationships were estimated using Bayesian inference (BI) implemented in MrBayes 3.2.7a (Ronquist et al., 2012). The Woodwardioideae ptDNA dataset was rooted using representatives of the family Onocleaceae as the outgroup. Each plastid DNA region was assigned the best-fitting substitution model. In case the best-fitting model was not implemented in MrBayes, the most similar implemented model was used. We ran MrBayes analyses with four coupled Markov Chains, one heated and three cold, using Metropolis-Hastings MCMC simulations, with one million generations per chain. A burn-in of 25% of the posterior probability sample was applied. The convergence of the chains was assessed by checking that the average standard deviation of split frequencies was below 0.01 (Ronquist et al., 2012), and that effective sample sizes were > 200 for all parameters with Tracer 1.7.2 (Rambaut et al., 2018). A 50% majority-rule consensus tree was then generated from the post-burn-in trees and visualised with FigTree 1.4.4 (Rambaut, 2018).

2.3. GBS library preparation and data assembly

Genotyping-by-sequencing libraries were prepared by the external service LGC Biosearch Technologies (Berlin, Germany) from 104 DNA samples digested with the restriction enzymes *Pst*I and *Ape*KI, following the protocol described in Poland et al. (2012). A total of 96 adaptors (each with a different barcode sequence) were designed for the first plate and eight for the second. These were ligated with the digested DNA fragments, each individual with a specific barcode. Subsequently, a common adaptor was hybridized to all samples. After combining all samples into a pool, the fragments were amplified by PCR. High-throughput sequencing (150 bp paired-end) of the resulting genomic library was performed on the Illumina NextSeq 500/550 v2 platform, followed by demultiplexing according to the barcodes. Demultiplexed data were deposited in the Sequence Read Archive (NCBI) under BioProject ID PRJNA1402703.

Data assembly and subsequent analyses were implemented on the Trueno scientific computing cluster (CSIC, Madrid, Spain). The assembly of loci was performed with *ipyrad* v. 0.9.84 (Eaton, 2014; Eaton and Overcast, 2020), a pipeline based on seven consecutive steps. Since data were already demultiplexed (step 1), we started by filtering and editing the reads, discarding sequences containing more than four sites showing a Phred quality value < 20, and removing adaptors and sequences shorter than 35 base pairs (step 2), followed by clustering within samples and alignment using VSEARCH (Rognes et al., 2016) and MUSCLE (Edgar, 2004) (step 3), joint estimation of error rates and heterozygosity (Lynch, 2008) (step 4), estimation of consensus sequences for each locus in each individual (base calling) and filtering of potential paralogs (step 5), clustering of sequences across samples and final alignment (step 6), and final filtering and generation of output files (step 7). We used parameters recommended for double-digest GBS libraries in the *ipyrad* documentation (https://ipyrad.readthedocs.io/en/master/7-outline.html), with two key modifications: for parameter 14 (c), the minimum percentage of similarity between sequences to consider them homologous, we tested threshold values of 85% and 90%, which are appropriate to cover the level of divergence between closely related species such as *W. radicans* and *W. unigemmata* (e.g. Fernández-Mazuecos et al., 2018; Rancilhac et al., 2023; Villanueva Raisman et al., 2025); for parameter 21 (m), which specifies the minimum number of individuals in which a locus must be recovered to be included in the final matrix, we initially used a value of 20. Other settings included: a maximum of one allowable mismatch in barcodes; a maximum of four low quality base calls (Q < 20) per read; a minimum depth for statistical base calling of six with no majority-rule base calling; a strict filter for adapters and primers; a minimum length of 35 bp for reads after adapter trim; a maximum of two alleles per site in consensus sequences (consistent with the established diploidy of *Woodwardia*: 2n = 68 in *W. radicans*, base chromosome number x ≈ 34 for the genus *Woodwardia,* and isozyme profiles indicative of diploidy; Löve et al., 1977; Quintanilla et al., 2007); a maximum of five uncalled bases in consensus sequences; up to eight heterozygous bases in consensus sequences; and a maximum of 50% of samples sharing heterozygous sites in a locus. Additionally, several samples displayed a small number of sequenced loci, which could introduce noise in the results. Specifically, samples of *W. radicans* from the Azores produced around 5,000 loci, compared to an average of 15,000 loci in the remaining samples. Therefore, alternative assemblies were built including and excluding the Azores samples. In the case of assemblies excluding Azores samples with m = 20, this parameter was decreased to 18. Similarly, herbarium samples outside of *W. radicans* generally produced small numbers of loci (e.g., fewer than 7,000 loci) and were very distant to *W. radicans* in preliminary analyses. This led us to retain *W. unigemmata*, consistently recovered as the closest relative of *W. radicans*, as the sole outgroup in the final datasets to ensure reliable rooting of the phylogenetic trees. To evaluate the sensitivity of results to variation in parameter m, we generated additional assemblies (including and excluding Azores samples) using c = 85% and m = 4, the latter value maximising the number of loci at the expense of a higher percentage of missing data. This optimization of assembly parameters is essential, as genetic results can be highly sensitive to them (Mastretta-Yanes et al., 2015; Shafer et al., 2015; Takahashi et al., 2014). As a result, six datasets were obtained: c85m4, c85m20, c90m20, including Azores; and c85m4, c85m18 and c90m18, excluding Azores (Table 2).

Table 2
Summary data sets used in the GBS analyses of *W. radicans*. Two clustering thresholds (0.85 and 0.90) were applied, with analyses both including and excluding samples from the Azores.

Data set	Clustering threshold	Number of loci	Average number of loci per individual	Concatenated length	Proportion of missing data	Number of variable sites	Number of phylogenetically informative sites
c85m4	0.85	41,258	14,321	8,440,461	64.38%	150,994	61,637
c85m4 (without Azores)	0.85	40,366	14,749	8,271,953	62.51%	145,795	59,859
c85m20	0.85	12,434	8,693	2,720,080	30.77%	54,477	26,781
c85m18 (without Azores)	0.85	13,768	9,628	2,994,995	30.4%	58,574	28,444
c90m20	0.90	15,035	10,325	3,262,170	31.94%	64,093	31,780
c90m18 (without Azores)	0.90	16,452	11,621	3,557,390	28.83%	68,189	33,421

2.4. Phylogenomics and population genomics

Phylogenomic analyses based on maximum likelihood (ML) were conducted using the six datasets. Maximum likelihood is generally more practical than Bayesian inference for analysing high-throughput sequencing datasets (Tonini et al., 2015), as it is computationally more efficient and particularly well suited for large matrices compared with Bayesian algorithms, which scale less favourably with genome-wide data (Stamatakis, 2014; Truszkowski et al., 2023). Additionally, it performs reliably in the presence of missing data as long as they are randomly distributed and a sufficient number of genes are sampled (Xi et al., 2016). Analyses were performed using the entire concatenated matrix rather than a single nucleotide polymorphism (SNP) matrix, as this approach is known to produce more accurate topologies and branch lengths (Leaché et al., 2015). ML analyses were carried out using RAxML 8.2.8 (Stamatakis, 2014). GTRCAT (Stamatakis, 2006) was chosen as the substitution model, and bootstrap support values were calculated using the bootstopping criterion (Pattengale et al., 2010). Samples of *W. unigemmata* were selected as the outgroup for rooting the tree.

The SNP matrix corresponding to the c85m20 dataset, which contained a total of 6,823 SNPs, was used to conduct a principal component analysis (PCA) of *W. radicans* samples, including and excluding the outgroup. These analyses were performed using Jalview 2.11.2.2 (Waterhouse et al., 2009). Genetic diversity of population groups and genetic differentiation between them were estimated using the software DnaSP v.6.12.03 (Rozas et al., 2017). The allele data file obtained from *ipyrad* v. 0.9.84 using the dataset c85m20 was used for these analyses. To determine which population genetic indices were most relevant, we followed the review by Pelosi and Sessa (2021), which evaluated studies on fern population genetics. Based on this, we calculated the fixation index (F_{ST}), a measure of population differentiation due to genetic structure (Hudson et al., 1992), where values above 0.25 indicate a pronounced level of genetic differentiation (Freeland et al., 2011). Additionally, we calculated nucleotide diversity (π), which represents the average number of differences per site among all possible sequence pairs within a population, reflecting its genetic diversity (Nei, 1987). A first analysis was conducted using Macaronesia and Western Palearctic as major population groups. Then, a more detailed analysis was performed using the following groups: Madeira, Canary Islands, Azores, NW Iberian Peninsula, and Mediterranean Basin (including Corsica, Italian Peninsula, Sicily, and Crete).

2.5. Fossil record, divergence times and ancestral ranges

We conducted a comprehensive bibliographic search for Woodwardioideae fossils using Google Scholar and two major fossil databases: the Laboratory of Palaeobotany (https://paleobotany.ru/) and the International Fossil Plant Names Index (https://www.ifpni.org/index.htm). The search was performed using the keywords Woodwardioideae, Blechnaceae, and *Woodwardia*. Although numerous fossils have been attributed to the Woodwardioideae subfamily, our focus was on identifying fossils that could provide critical information for dating the phylogeny of the subfamily. Additionally, we sought fossils of *Woodwardia* located within the present-day range of disjunction for the *W. radicans–W. unigemmata* lineage (see Table 3).

Divergence times were estimated in two steps. First, we estimated a dated tree from the Woodwardioideae ptDNA dataset. Subsequently, we constructed a second dated tree for intraspecific lineages of *W. radicans* derived from a ML tree obtained from the GBS dataset and calibrated using divergence times from the dated Woodwardioideae ptDNA tree. The Woodwardioideae ptDNA dataset was analyzed using the Bayesian molecular clock methods implemented in BEAST 1.10.4 (Drummond et al., 2006; Suchard et al., 2018). The BEAST input file was generated using BEAUti 1.10.4 (Suchard et al., 2018), and the GTR + G + I substitution model was selected based on model selection in jModelTest. For the relaxed clock model, an uncorrelated lognormal distribution was applied, fitted to values commonly observed in plastid markers (a mutation rate between 10^{-4} and 10^{-1} substitutions per site per million years; Wolfe et al., 1987), together with a default exponential distribution for ucld.stdev. Two dating analyses were conducted to identify the tree prior model that best fitted our data: one using the Yule model, which only considers speciation (Gernhard, 2008), and another using a Birth–Death (BD) model, which incorporates both speciation and extinction (Gernhard, 2008). To assess which of the two tree priors best fitted our plastid dataset, we compared the Yule and Birth–Death models using path sampling and stepping-stone sampling (Baele et al., 2012). As calibration points, we used two secondary calibrations derived from the most comprehensive dating analysis available for the family Blechnaceae (Testo et al., 2022) and two fossils corresponding to the subfamily Woodwardioideae (see above; Table 3): i) a secondary calibration for the divergence between Onocleaceae and Blechnaceae (normal distribution; mean = 90.14 Ma, standard deviation (sd) = 9); ii) a secondary calibration for the crown node of Blechnaceae (normal distribution; mean = 73.78 Ma, sd = 6); iii) a fossil corresponding to the genus *Lorinseria* (Pigg et al., 2006), which marked the minimum age of the divergence between the genus *Lorinseria* and *Woodwardia* plus *Anchistea* (log-normal distribution; offset = 56 Ma, sd = 2.5); and iv) a fossil of *W. radicans* (Góis-Marques et al., 2018), which marked the minimum age of the divergence between *W. radicans* and *W. unigemmata* (log-normal distribution; offset = 1.8 Ma, sd = 2.5). This fossil shows anastomosed venation, a prominent costa, and oblong sori arranged parallel to the costa—diagnostic features of *Woodwardia* and consistent with *W. radicans*. However, the available morphological evidence does not allow us to confirm whether it belongs to the crown group included in our phylogeny (i.e. modern Macaronesian and continental populations). For this reason, we conservatively assigned it to the stem divergence between the two sister species, following best-practice guidelines for fossil calibration (Donoghue and Benton, 2007; Parham et al., 2012; Renner, 2005). Standard deviations were assigned and adjusted to align with the confidence intervals for each calibration. Two input files were generated,

Table 3
Fossil record of Woodwardioideae species from the Paleocene to Pliocene epochs, including their age, locations, and references. The table highlights occurrences of *Woodwardia muensteriana*, *W. roessneriana*, and *W. radicans* across Europe and Central Asia.

Species	Epoch	Age (Ma)	Location	Latitude	Longitude	Reference
Lorinseria areolata (L.) T.Moore	Late Paleocene	59.2–56	Western North Dakota	47.5	−100.5	Pigg et al., 2006
Woodwardia muensteriana (C.Presl in Sternb.) Kräusel	Early Miocene	23.03–15.97	Most Basin, Czech Republic	50.5	14	Kvaček et al., 2018
Woodwardia muensteriana (C.Presl in Sternb.) Kräusel	Late Miocene	11.63–5.33	Belo Pole, Bulgaria	43.13	22.43	Palamarev et al., 2005
Woodwardia muensteriana (C.Presl in Sternb.) Kräusel	Late Miocene	11.63–5.3	Pelovo, Bulgaria	43.573	23.633	Palamarev et al., 2005
Woodwardia muensteriana (C.Presl in Sternb.) Kräusel	Late Miocene	11.63–5.3	Rouzhintsi, Bulgaria	43.65	23.45	Palamarev et al., 2005
Woodwardia muensteriana (C.Presl in Sternb.) Kräusel	Middle Miocene	15.97–11.63	Choukourovo, Romania	44.433	25.657	Palamarev et al., 2005
Woodwardia roessneriana (Unger) Heer	Middle Miocene	15.97–11.63	Radoboj, Croatia	46.333	16.067	Heer, 1855-1859
Woodwardia muensteriana (C.Presl in Sternb.) Kräusel	Middle Miocene	15.97–11.63	Bohemia, Czech Republic	50	14.44	Collinson, 2001
Woodwardia muensteriana (C.Presl in Sternb.) Kräusel	Middle Miocene	15.97–11.63	Saxony, Germany	51.05	13.74	Collinson, 2001
Woodwardia muensteriana (C.Presl in Sternb.) Kräusel	Early-Middle Miocene	23.03–11.63	Caucasus	43	45	Collinson, 2001
Woodwardia roessneriana (Unger) Heer	Early-Middle Miocene	23.03–11.63	Eriz, Switzerland	46.813	8.305	Heer, 1855-1859
Woodwardia radicans (L.) Sm.	Late Miocene – Early Pleistocene	7–1.8	Madeira, Portugal	32.76	−16.934	Góis-Marques et al., 2018
Woodwardia muensteriana (C.Presl in Sternb.) Kräusel	Oligocene	33.9–23.03	Kazakhstan	48	67	Il'inskaya and Pneva, 1984
Woodwardia radicans (L.) Sm.	Pliocene	5.33–2.58	Meximieux, France	45.9	5.225	Saporta et al., 1872

each implementing a different tree prior model, and each analysis was run for 10 million generations, with sampling every 1,000 generations. Tracer 1.7 (Rambaut et al., 2018) was used to verify posterior distributions and ensure that effective sample size (ESS) values were > 200. A burn-in of 20% was applied before calculating a maximum clade credibility (MCC) tree using TreeAnnotator 1.10.4 (Rambaut and Drummond, 2018). The resulting chronogram was visualised in FigTree (Rambaut, 2018).

Since Bayesian dating is unfeasible with genome-wide GBS data due to computational limitations, we dated the intraspecific lineages of *W. radicans* using the penalised likelihood approach implemented in treePL (Smith and O'Meara, 2012). As input file, we used the ML phylogram obtained in RAxML from the GBS dataset c85m18 (see results), i.e. excluding Azores individuals. The tree was pruned to include only one arbitrarily selected individual per geographic area/island, prioritizing populations with supported relationships in the phylogenetic reconstruction. Two secondary calibration points were derived from the dated tree constructed with the Woodwardioideae ptDNA dataset (see results): the crown node of the genus *Woodwardia*, with an estimated age range of 13.66 to 28.43 Ma, and the divergence between *W. radicans* and *W. unigemmata*, with an age range of 1.85 to 4.64 Ma. A first analysis was conducted using the *prime* option to determine optimal parameter values. Based on these results, a second analysis was performed using the cross-validation option to identify the best smoothing parameter, which was determined to be 1×10^{-10}. In all cases, the exhaustive analysis option was applied, with 200,000 iterations for penalised likelihood and 5,000 iterations for cross-validation. To assess uncertainty in node ages, two additional estimations were performed, each following the three steps outlined above: one for calculating minimum values and another for maximum values. In both cases, the corresponding calibration ages were used, meaning that the minimum and maximum values from the Woodwardioideae ptDNA tree were applied as calibration ages for their respective calculations. The smoothing value varied between analyses: 0.01 was used for the minimum ages, while 1×10^{-11} was applied for the maximum ages. The resulting chronograms were visualised in FigTree.

To reconstruct ancestral ranges and dispersal patterns, we applied the Bayesian Island Biogeographic (BIB) model (Sanmartín et al., 2008; Aguado-Lara et al., 2025), a hierarchical Bayesian framework linking biogeographic and molecular data through a continuous-time Markov Chain process. Migration rates between regions were estimated via MCMC using DNA sequence data and taxon distributions. Analyses were performed in RevBayes (Höhna et al., 2016), with predefined molecular characters and Dirichlet priors ($\alpha = 1.0$) assigned to carrying capacities and dispersal rates to reflect uncertainty. We defined four biogeographic areas based on the distribution of the *W. radicans–W. unigemmata lineage*: Eastern Palearctic (EP), Mediterranean Basin (MED), Atlantic Iberia (AI), and Macaronesia (MAC). Outgroup taxa were removed, and biogeographic states were coded for the BIB model. MCMC was run for 100,000 generations (sampling every 10), with a gamma prior on root age based on BEAST estimates. Posterior probabilities of ancestral and branch states were computed using stochastic mapping (Freyman and Höhna, 2018). Summaries were derived from the Maximum A Posteriori (MAP) tree, discarding a 25% burn-in. Results were visualized in R (v4.1.2) using the *base*, *graphics*, *coda*, *RevGadgets* (Tribble et al., 2022), and *ggplot2* (Wickham, 2016) packages, as well as Tracer.

2.6. Environmental niche modelling

By reconstructing the climatic niches of the *W. radicans–W. unigemmata* lineage and projecting them backward in time, we aimed to identify climatically suitable areas that might have been part of the geographic distribution or served as climatically suitable areas or refugial connectivity routes (Yesson and Culham, 2006; Smith and Donoghue, 2010; Mairal et al., 2015). Occurrence data for *W. radicans* and *W. unigemmata* were downloaded from the Global Biodiversity Information Facility (GBIF) (accessed 9 March 2023; GBIF Occurrence Download: https://doi.org/10.15468/dl.8u79bu) and processed using the R package CoordinateCleaner 3.0.1 (Zizka et al., 2019). A general cleaning of the data was performed following Maldonado et al. (2015), resulting in a total of 3,873 points for *W. radicans* and 840 for *W. unigemmata*. To mitigate sampling bias, a minimum distance of 2 km between points was established to reduce spatial autocorrelation, consistent with the resolution of the environmental layers (Kramer-Schadt et al., 2013; Boria et al., 2014), and finally an individual cleaning using QGIS 3.12 (QGIS Development Team, 2020) yielded a final set of 130 points for *W. radicans* and 153 for *W. unigemmata*.

Climate layers were obtained from CHELSA 2.1 (Karger et al., 2017), at a resolution of 5 km. For projections to the past, we used climate layers for various periods from PaleoClim (https://www.paleoclim.org):

the mid-Pliocene warm period (3.205 Ma), the Marine Isotope Stage 19 (MIS 19, 787,000 years ago; Brown et al., 2018), the Last Interglacial (130,000 years ago; Otto-Bliesner et al., 2006), the Last Glacial Maximum (21,000 years ago; Karger et al., 2017), the mid-Holocene (Northgrippian Stage, 8,326 to 4,200 years ago), and the late-Holocene (Meghalayan Stage, 4,200 to 300 years ago). Prior to modelling, a correlation analysis between the current climate layers was conducted using the R package *corrgram* (Wright, 2018) for a sample of 30,000 points from an area spanning the distribution ranges of *W. radicans* and *W. unigemmata* (from 35° W to 160° E longitude and from 11° to 70° N latitude), including presence and absence points. Correlations among climate variables were assessed, and when two variables were highly correlated (Pearson's correlation coefficient $\geq$ 0.8), one of them was excluded, leading to a final set of six uncorrelated variables for model calibration: annual mean temperature (bio1), minimum temperature of the coldest month (bio6), mean temperature of the wettest quarter (bio8), annual precipitation (bio12), precipitation seasonality (bio15) and precipitation of the coldest quarter (bio19). These variables represent the main climatic gradients relevant to *W. radicans* (temperature, precipitation, and seasonality). The use of non-correlated predictors follows standard best practices to minimise model overfitting and enhance transferability (Elith et al., 2011; Dormann et al., 2013).

Two modelling approaches were implemented: i) a combined analysis, in which distribution data for both *W. radicans* and *W. unigemmata* were included (283 points), focusing on an area spanning from 35° W to 160° E longitude and from 11° to 70° N latitude; and ii) a *W. radicans* analysis (130 points), focusing on an area spanning from 36° W to 45° E longitude and from 23° to 53° N latitude. We note that the combined analysis is not intended to infer a shared or ancestral niche, but rather to approximate a broad climatic envelope representing the environmental space historically accessible to the post-boreotropical, paleotropical-affinity *Woodwardia* lineage in Eurasia. Environmental niche models and projections to the past were carried out using *MaxEnt* 3.4.4 (Phillips, Anderson and Schapire, 2006). Each model was run with ten cross-validated replicates, using 25% of the samples for validation. Model accuracy was assessed using AUC and omission rates, which indicated high predictive performance (Fig. S1). The combined *W. radicans–W. unigemmata* model was projected to the mid-Pliocene warm period, which was close to the common ancestor of the two species (see Results). Variable bio6 was excluded from this model because it was not available for the mid-Pliocene. The *W. radicans* analysis involved projections to time slices ranging from the MIS 19 to the present, when the species had already diverged from *W. unigemmata*. For the MIS 19 projection, a model was run excluding variable bio6 because it was not available for this period. For the remaining projections, the model included all six selected variables.

3. Results

3.1. Phylogenetic relationships and divergence times of Woodwardioideae

The Woodwardioideae ptDNA matrix consisted of 4,976 base pairs. Model selection in jModelTest 2.1.10 (Darriba et al., 2012) indicated GTR + G as the best-fitting nucleotide substitution model for the analysis. The phylogenetic tree obtained in MrBayes from this dataset generally shows high resolution and support values (Fig. 2). The subfamily Woodwardioideae was identified as the sister group to a clade including the subfamilies Stenochlaenoideae and Blechnoideae. Within the subfamily Woodwardioideae, *Lorinseria* was positioned as the earliest-diverging genus followed by *Anchistea*. The latter genus was sister to *Woodwardia*, which formed a monophyletic group. Within *Woodwardia*, *W. unigemmata* and *W. radicans* were sisters to each other. All these relationships exhibited posterior probabilities (PPs) above 0.95.

The dated MCC trees obtained from the BEAST analyses of the Woodwardioideae ptDNA dataset (Fig. 3) were topologically congruent with the MrBayes tree (Fig. 2). The analyses using the Yule and the BD priors yielded congruent divergence times and posterior probabilities. Model comparison using path sampling and stepping-stone sampling showed that the Yule and BD priors had nearly identical marginal likelihoods (Bayes factors < 2), indicating no statistical preference for either model. Given this equivalence, and because the BD prior represents a more biologically realistic diversification process for *Woodwardia*, we present the divergence-time estimates obtained under the BD model

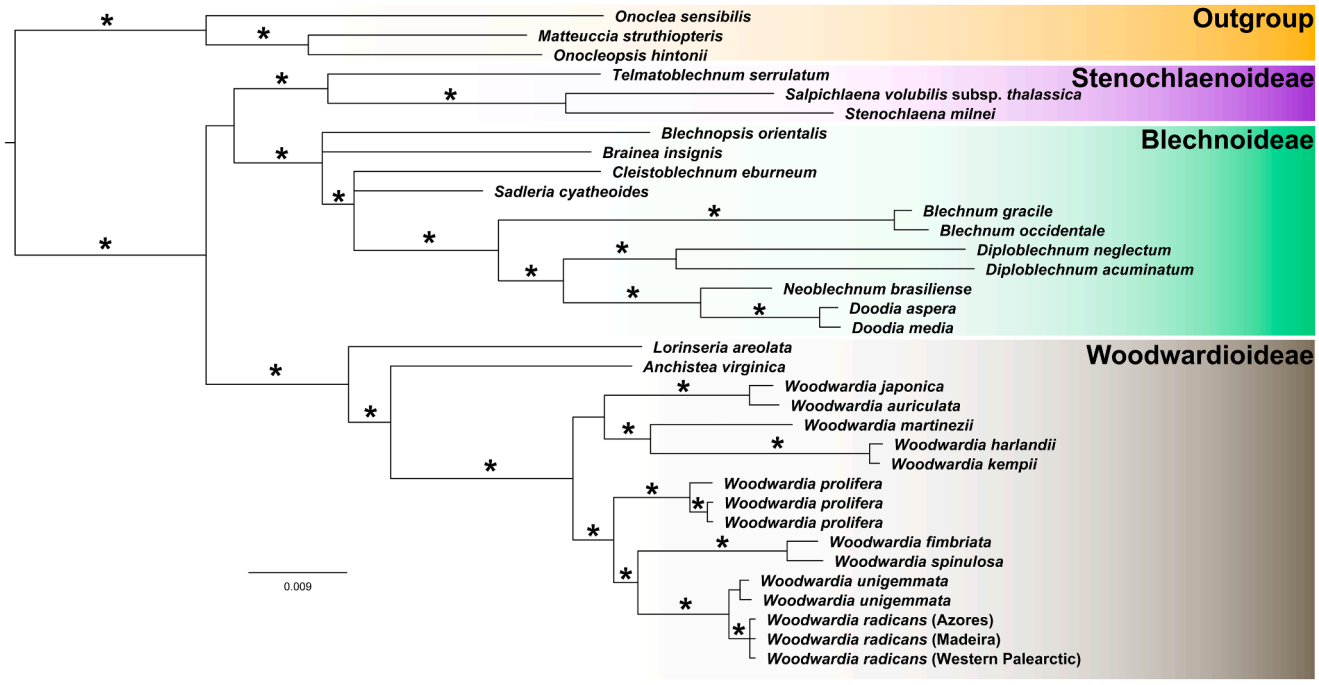

Fig. 2. Bayesian majority-rule consensus tree obtained in MrBayes from the Woodwardioideae ptDNA dataset (*rps*4, *rbc*L, *atp*B, *mat*K). Asterisks above branches indicate Bayesian posterior probabilities above 0.95.

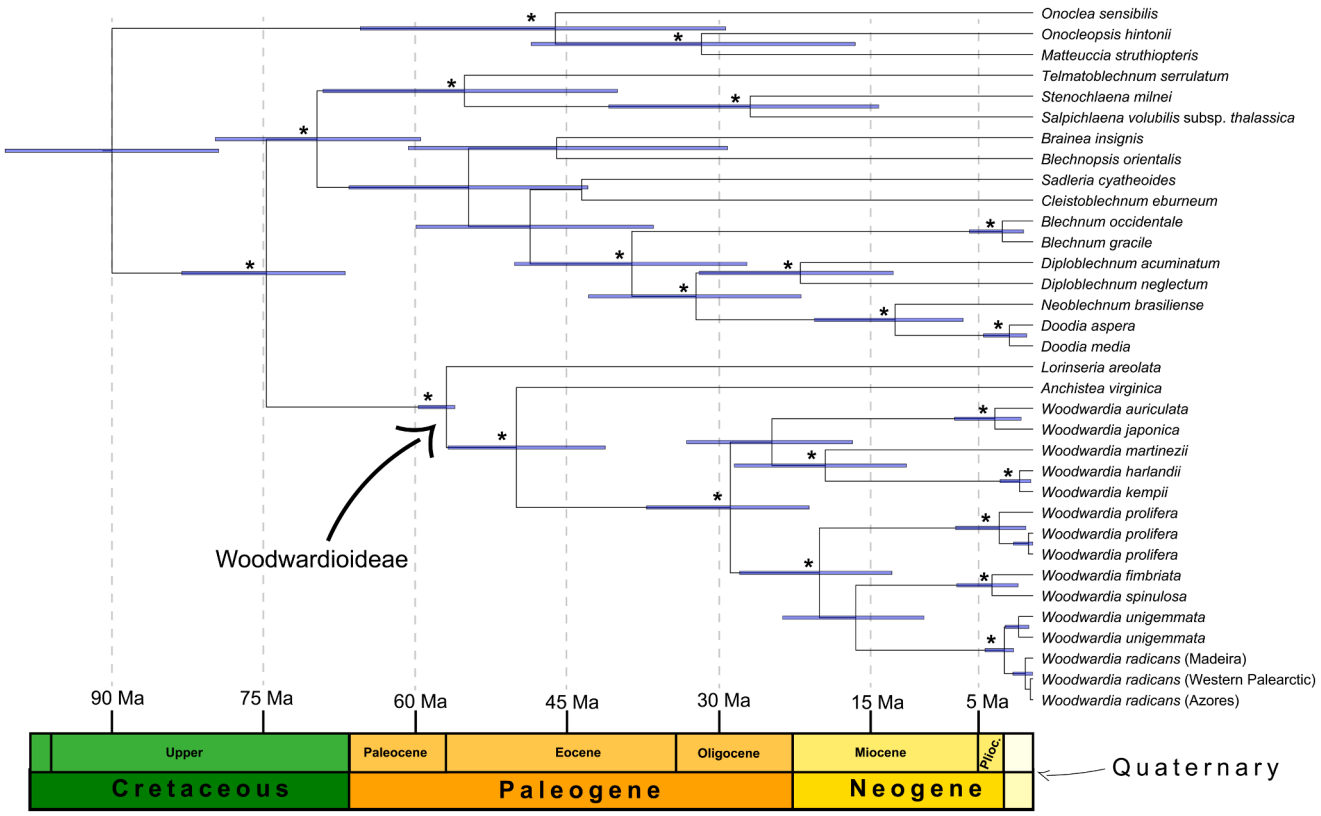

Fig. 3. Maximum clade credibility tree obtained in BEAST from the Woodwardioideae ptDNA dataset, with 95% highest posterior density intervals for divergence times. Asterisks above branches indicate Bayesian posterior probabilities above 0.95.

(Fig. 3, Fig. S2). Divergence of Woodwardioideae and the rest of the Blechnaceae family was dated to the Late Cretaceous (74.31 Ma, 95% highest posterior density (HPD) = 66.66–82.52 Ma; PP = 1). The crown node of the subfamily Woodwardioideae was dated to the Paleocene

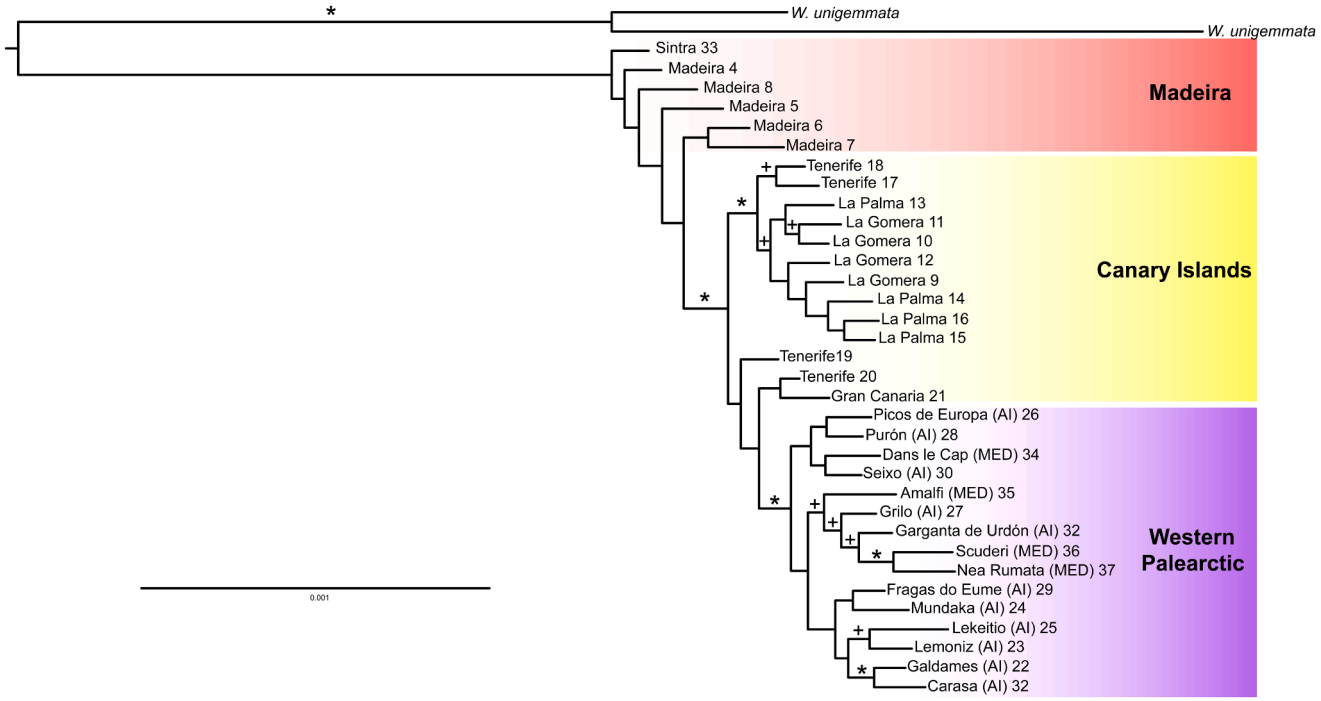

Fig. 4. Concatenation-based maximum-likelihood phylogenetic tree of *Woodwardia radicans* populations obtained in RAxML using GBS data (c85m18 dataset; excluding samples from the Azores), with *W. unigemmata* as the outgroup. Asterisks (*) indicate nodes with bootstrap support values (BS) ≥ 95, while plus signs (+) indicate nodes with 70 ≤ BS < 95. The letters within parentheses show the regions: AI: Atlantic Iberia, C: Corsica, I: Italy, S: Sicily and Cr: Crete. Numbers correspond to each population, with codes provided in Table 1.

(58.86 Ma, 95% HPD = 56.03–59.57 Ma; PP = 1). The crown node of *Woodwardia* was dated to the late Eocene–early Miocene (29.33 Ma, 95% HPD = 21.69–37.46 Ma; PP = 1). The divergence between *W. radicans* and *W. unigemmata* was dated to the Pliocene or early Pleistocene (2.76 Ma, 95% HPD = 1.85–4.64 Ma; PP = 1), whereas crown ages were dated to the late Pliocene or Pleistocene for *W. unigemmata* (1.38 Ma, 95% HPD = 0.38–2.66 Ma; PP = 0.98) and to the Pleistocene for *W. radicans* (0.73 Ma, 95% HPD = 0.02–1.92 Ma; PP = 1).

3.2. Phylogenomics, population genomics, divergence times and ancestral ranges in W. radicans

For the four assembled datasets with m values of 18–20, the resulting number of loci ranged from 12,000 to 16,500, resulting in concatenated matrices ranging from 2.7 to 3.6 million base pairs (Table 2). The percentage of missing data was around 30%. For the two datasets with m = 4, the number of loci was around 40,000, with a concatenated length of > 8 million base pairs and > 60% of missing data.

The ML phylogenetic analysis of the c85m18 dataset, in which Azores samples were excluded, displayed the best resolution and support values (Fig. 4). This tree revealed an early-diverging position for the Madeira populations and the introduced Sintra (Portugal) population, with unsupported relationships among them, and the remaining populations (Canary Islands and Western Palearctic) forming a strongly supported clade (bootstrap support, BS = 99%). This clade was further divided into two well-supported and geographically structured clades: one comprised populations from the central-western Canary Islands (Tenerife, La Palma and La Gomera; BS = 97%), while the other included Western Palearctic populations (BS = 100%). Three populations from the central Canary Islands (Tenerife and Gran Canaria) displayed uncertain relationships and were grouped with the Western Palearctic clade with low support. Therefore, the Western Palearctic populations formed a monophyletic group nested within the Macaronesian populations, making the latter a paraphyletic assemblage. Within the Western Palearctic clade, populations from the eastern Mediterranean continental islands (Sicily and Crete) were nested within the Western Palearctic populations (closely related to Atlantic Iberia populations) and formed a clade with strong support (BS = 100%). The ML analyses of the four datasets generated with m values of 18–20 (Table 2) produced the same overall topology, with some minor variations. In the analyses including the Azores populations, these were well supported as being part of the clade encompassing populations from the Canary Islands and Western Palearctic (BS = 88% for the c85m20 dataset; Fig. S3), but with unsupported relationships within this clade. In the ML analyses of the two datasets generated using m = 4, the overall relationships were similar, but with weaker support at some key nodes, which led us to discard these datasets for downstream analyses (results not shown).

The PCA based on the c85m20 dataset displayed a clear differentiation between *W. radicans* and *W. unigemmata*, forming two distinct, non-overlapping clusters along the principal components (Fig. S4). Within *W. radicans*, the PCA also revealed differentiation between Macaronesian and Western Palearctic populations (Fig. 5), particularly along PC2, with Macaronesian populations (including the introduced Sintra population, 33) showing higher values than Western Palearctic ones. Among Macaronesian populations, those from the Canary Islands and Madeira displayed a high level of dispersion along PC1, while Azores populations displayed the highest values for this PC. Among Western Palearctic populations, those from Atlantic Iberia and Mediterranean continental islands clustered closely together at small values of both PC1 and PC2, with the exception of the Corsica population (34), which exhibited higher values for both PCs and was close to some Azores and Canary Island populations, possibly due to their high levels of missing data (Fig. 5). The DnaSP analysis estimated higher nucleotide diversity (π) for Macaronesian (0.00063) than for Western Palearctic (0.00051) populations. Similarly, when considering five population

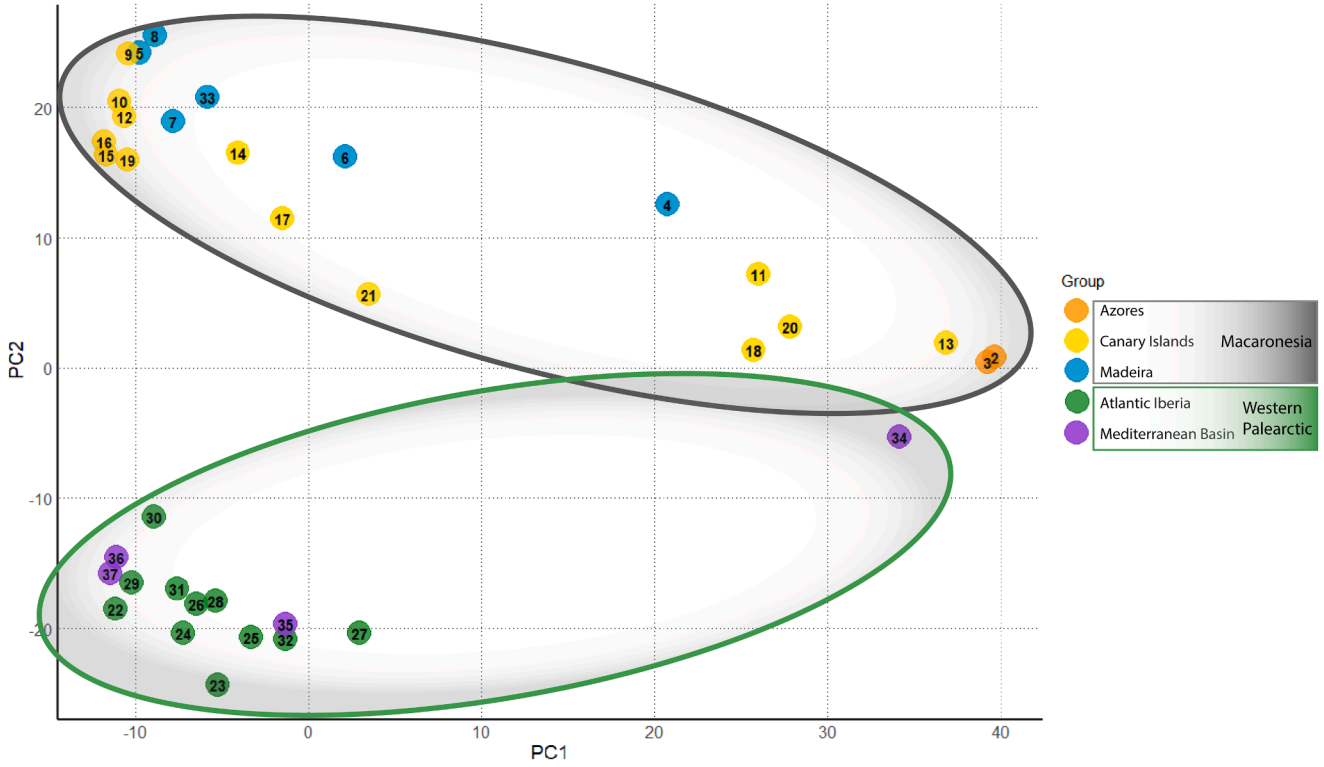

Fig. 5. Principal component analysis plot based on SNPs obtained by genotyping-by-sequencing (GBS) of *Woodwardia radicans* samples, showing genetic variation among geographic regions. PC1 and PC2 represent the first two components, explaining 48.7% and 9.5% of the variance, respectively. Each point represents an individual from a different population, numbered as in Table 1, with colors indicating geographic origin as shown in the legend.

groups, Madeira, Azores and Canary Island populations displayed higher nucleotide diversity than Mediterranean Basin and NW Iberian Peninsula populations, with Madeiran populations displaying the highest diversity and NW Iberian populations the lowest (Table S2). Genetic differentiation between these two major regions, as measured by the F_{ST} index, was 0.0557, indicating moderate genetic differentiation. When considering five population groups, the lowest differentiation values were found between the three pairs of Macaronesian archipelagos, while the highest values were found between Mediterranean Basin populations and those from Madeira and the Canary Islands (Table S3).

The chronogram obtained in treePL from the GBS phylogram (Fig. 6) showed a crown age for *W. radicans* in the Pleistocene, around 0.57 Ma (0.38–0.66 Ma). After the divergence of the Madeiran populations, the common ancestor of populations in the Canary Islands and the Western Palearctic had an estimated age of 0.35 Ma (0.27–0.47 Ma). The estimated crown age of Canarian populations was 0.26 Ma (0.17–0.33 Ma), while that of Western Palearctic populations was 0.27 Ma (0.19–0.36 Ma).

The BIB reconstruction of the *W. radicans–W. unigemmata* lineage inferred a range for the most recent common ancestor (Fig. 6) with low marginal posterior probabilities across the defined biogeographic areas (MAC = 0.29; MED = 0.24; AI = 0.24). These values indicate substantial uncertainty at this deeper node, and therefore no single ancestral area can be reliably inferred. Within the Western Palearctic clade (crown age: 0.57 Ma), Macaronesia was identified as the most probable ancestral area, with moderate support (MAC = 0.76; AI = 0.15; MED = 0.05). Macaronesia probably acted as the ancestral source region for Atlantic Iberia (AI) around 0.35 Ma (MAC = 0.71; AI = 0.23), although some uncertainty remains regarding the exact timing and directionality of this range shift. Subsequently, Atlantic Iberia was the most likely ancestral area for at least three dispersal events to the Mediterranean Basin over the last 0.27 Ma (AI = 0.92; MED = 0.06).

3.3. Environmental niche modelling

The average AUC values for the models, ranging between 0.975 and 0.996 (standard deviation between 0.002 and 0.008), together with test omission rates being close to predicted omission, indicated good predictive performance (Fig. S1). For the *W. radicans–W. unigemmata* model, the variables with the highest percent contributions were bio1

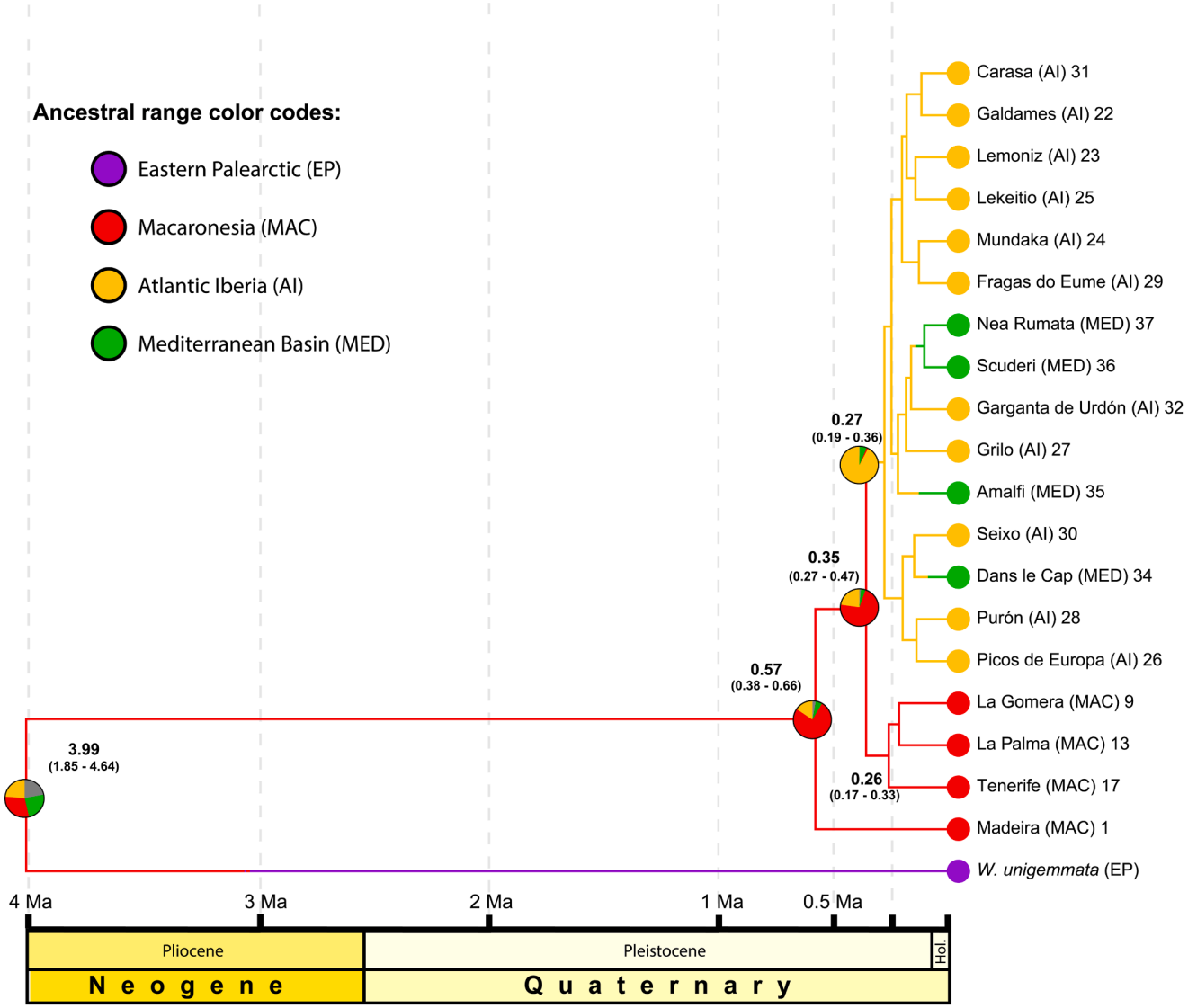

Fig. 6. Time-calibrated phylogenetic tree and ancestral range reconstruction of *Woodwardia radicans*, obtained with treePL from a pruned RAxML tree based on GBS data and using the BIB model (Bayesian Island Biogeography). Nodes are labeled with mean divergence ages (Ma), with minimum–maximum estimates in parentheses. Pie charts at the nodes show the marginal posterior probabilities of ancestral geographic ranges (see legend for colors). Marginal posterior probabilities for dispersal events along branches, estimated via stochastic character mapping, are represented by colors according to the legend.

(52.4%) and bio12 (29.6%). For the *W. radicans* model including all six variables, the ones with the highest contributions were bio19 (42.7%), bio6 (25.1%) and bio1 (21.8%). When excluding bio6, they were bio19 (53.3%) and bio1 (27.7%). Projection of the combined *W. radicans–W. unigemmata* model to the mid-Pliocene warm period (Fig. 7a; 3.205 Ma) revealed a broad potential distribution range, with high suitability along a discontinuous latitudinal band extending from eastern Asia to the western Mediterranean, with patchy high-suitability areas across these regions. This includes widespread suitability in Europe, the Eastern African Rift Mountains, and parts of Asia, particularly in the east of the Black Sea and the Himalayas. Projections of the *W. radicans* model in the Western Palearctic (Fig. 7b–g) indicated suitable conditions for its persistence throughout the late Quaternary, but with reduced suitability and increased fragmentation compared to the mid-Pliocene potential distribution (Fig. 7a). During the MIS 19 (Fig. 7b), the potential distribution was notably fragmented, and primarily restricted to the northern Mediterranean Basin and the Iberian Atlantic coasts. In Macaronesia, suitability was found in the Azores, Madeira and, to a lesser extent, the Canary Islands. Habitat suitability further declined leading up to the Last Interglacial (Fig. 7c), particularly

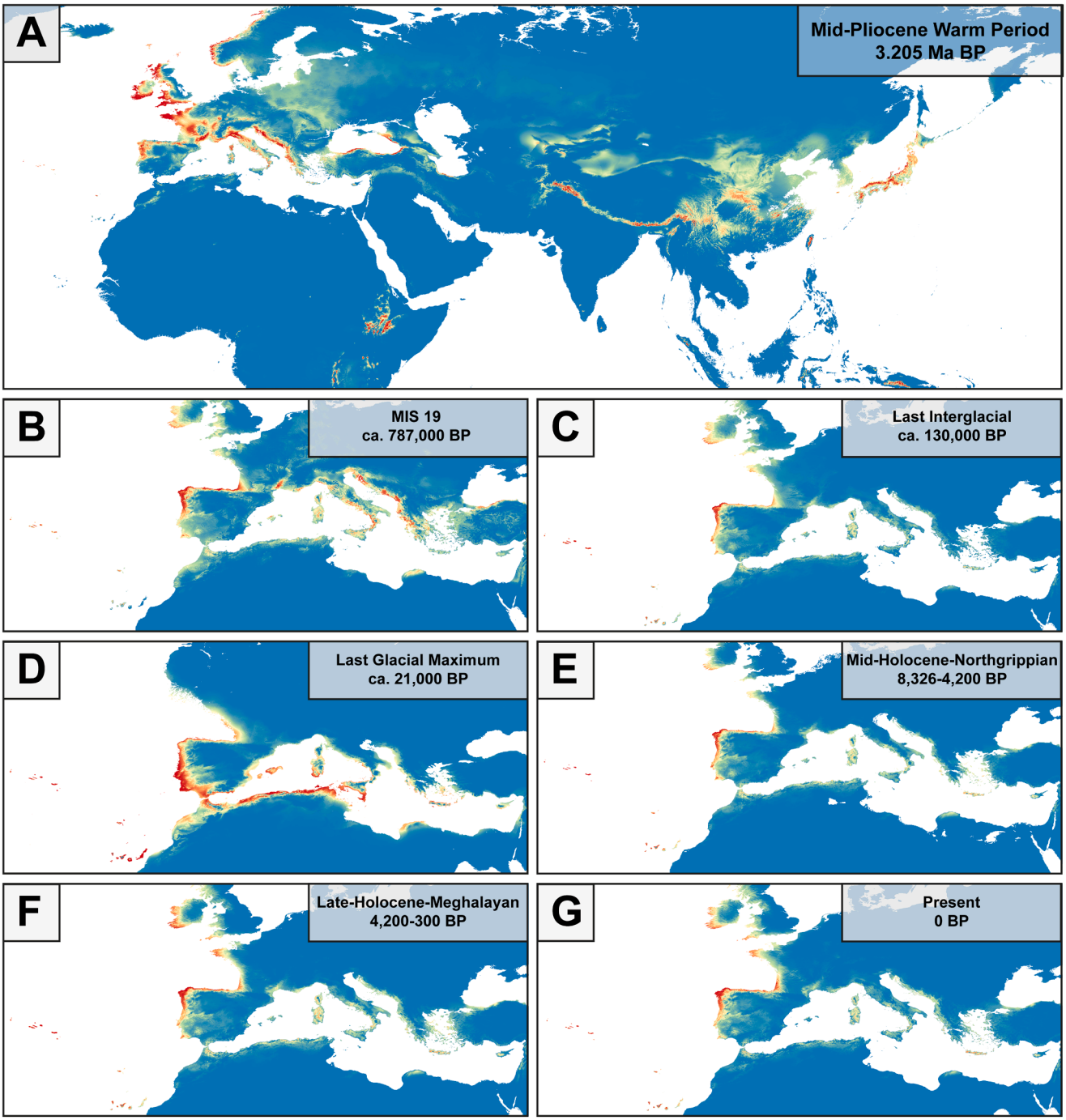

Fig. 7. Environmental niche modeling for *Woodwardia radicans* in the Mediterranean Basin based on climatic variables. Environmental suitability is shown for six historical time periods (A-F) and the present (G), as predicted by maximum entropy modeling. The color gradient ranges from cool to warm, indicating areas of low suitability in cooler tones and regions of higher suitability in warmer tones. Projection A corresponds to the *W. radicans*−*W. unigemmata* model, while projections B-G correspond to the *W. radicans* model.

in the Mediterranean coasts, although it increased in the Canary Islands. During the Last Glacial Maximum (Fig. 7d), suitability declined at higher latitudes, while increasing at lower latitudes, particularly in northern Africa. During the Holocene, the potential distribution contracted again and became largely confined to the Macaronesian archipelagos, the Atlantic coasts of western Europe and, to a lesser degree, the coast of the Mediterranean Basin (Fig. 7e–g).

4. Discussion

4.1. Tracing intracontinental vicariance across Eurasia: Woodwardia and the legacy of the paleotropical belt

Our phylogenetic reconstruction for Blechnaceae (Fig. 2) reveals a topology consistent with the most comprehensive phylogenetic studies available for the family (Gasper et al., 2017; Testo et al., 2022), confirming the sister relationship between the subfamily Woodwardioideae and a clade including the subfamilies Stenochlaenoideae and Blechnoideae, as well as the monophyly of the genus *Woodwardia*, which is also confirmed as sister to the monotypic genus *Anchistea* (Fig. 2).

The current disjunct distribution of *Woodwardia* across continents has been hypothesized to result from the existence of an ancient paleotropical vegetation belt in the Northern Hemisphere (Mai, 1989, 1991)—also termed the boreotropical flora sensu Mai (1989, 1991)—that extended across the Northern Hemisphere during the early Cenozoic. Under this scenario, Asia, Europe, and North America would have experienced biotic exchange during the early to mid-Cenozoic, enabled by broad-scale climatic connectivity and intermittent land bridges. This would be reflected in reciprocal monophyly among lineages from different continents, as well as deep divergence times coinciding with the progressive fragmentation of these corridors from the Miocene onward. Our results support this scenario: we found reciprocal monophyly between *Woodwardia* lineages from Asia and America. One lineage includes the Central American *W. martinezii* Maxon ex Weath. as sister to the Asian *W. harlandii* Hook. and *W. kempii* Copel., diverging during the Oligocene–Miocene (20.13 Ma, 95% HPD = 12.26–28.94; Fig. 3). Similarly, the Eurasian clade *W. radicans*–*W. unigemmata* is sister to the American clade *W. fimbriata* Sm. – *W. spinulosa* M.Martens & Galeotti, with a divergence time of 17.16 Ma (95% HPD = 10.54–24.26; Fig. 3), although this relationship shows lower support (PP = 0.95). An alternative topology recovered by Testo et al. (2022) placed these American species closer to other Asian taxa (*W. magnifica*, *W. prolifera*, *W. orientalis*), but still reflected a clear biogeographic connection between Asia and America. These patterns, along with warmer temperatures during the Mid-Miocene Climatic Optimum (MMCO, 17–14 Ma; Beerling et al., 2012), are consistent with a period of increased biotic exchange between Asia and America. Similar connections have been documented in numerous Northern Hemisphere plant and animal lineages (Donoghue et al., 2001; Sanmartín et al., 2001; Wen et al., 2016), likely facilitated by the Bering Land Bridge (Hsu, 1983; Tiffney and Manchester, 2001; Lee et al., 2020). This dispersal route was especially important for paleotropical floras, including ferns (Sigel et al., 2014; Xiang et al., 2015; Molino et al., 2019), and likely facilitated the early diversification and dispersal of ancestral *Woodwardia* lineages.

Additionally, we confirm the reciprocal monophyly of *W. radicans* and *W. unigemmata* across a major Eurasian disjunction, which originated in the Plio-Pleistocene (2.76 Ma, 95% HPD = 1.85–4.64 Ma, Fig. 3; 3.99 Ma, 95% HPD = 1.85–4.64 Ma; Fig. 6). This pattern aligns with the fragmentation of a previously more continuous distribution caused by aridification, leaving relict populations of paleotropical-affinity taxa at the eastern and western ends of that geographic range (Mairal et al., 2015, 2017). This is further supported by fossil evidence and niche modelling, indicating the historical presence of *Woodwardia* populations in intermediate areas bridging the current geographic ranges of these extant sister species (Collinson, 2001). Specifically, *Woodwardia* fossils dating from the Oligocene to the Pliocene have been found in intermediate areas of central Europe and Georgia (Fig. 1a; Table 3). The *Woodwardia* fossil record, however, is geographically biased, with numerous occurrences in central and western Europe but few from the eastern Palearctic. This pattern likely reflects a combination of preservation and collection biases, rather than a genuine absence of the lineage in eastern regions. Moreover, due to the morphological conservatism of fern fronds and sori, the assignment of fossils to species must be interpreted cautiously, as diagnostic features are not always preserved. In addition to fossil evidence, the environmental niche model for the mid-Pliocene warm period (ca. 3.205 Ma; Fig. 7) reveals a broad potential distribution for the *W. radicans*–*W. unigemmata* lineage, spanning Europe, North Africa, and parts of Asia. This combined model represents a broad climatic envelope for the lineage rather than a shared niche of the two species. Although this reconstruction does not support the existence of a continuous vegetational belt across the continent, it points to the presence of patchy climatically suitable areas that may have functioned as stepping-stones for *Woodwardia* dispersal between the eastern and western extremes of Eurasia, before being disrupted by progressive aridification and cooling (Klotz et al., 2006). As with any paleoclimatic ENM, these projections must also be interpreted with caution due to uncertainties in past-climate reconstructions, including the use of single-GCM layers, CO_2 estimates, and the assumption of long-term niche stability (Varela et al., 2011; Nogué et al., 2017).

In summary, the current distribution of the Woodwardioideae in Eurasia, confined to the extremes of the continent, is consistent with a historical scenario dominated by range fragmentation and survival in refugial remnants of the former paleotropical (lauroid) vegetation belt. An ancestral *Woodwardia* species was likely widespread throughout the paleotropical belt in Eurasia during the early Cenozoic. As climate changes caused the retreat of this vegetation, surviving populations were forced to migrate toward southern latitudes, finding refuge in continental margins or nearby archipelagos with milder climates (Barrón, 2003; Fernández-Palacios et al., 2011; Vanderpoorten et al., 2007). The extinction of intermediate populations across Eurasia disrupted connectivity between eastern and western lineages, with subsequent persistence and limited post-boreotropical stepping-stone colonization shaping the divergence between them. This combination of vicariance, episodic dispersal, and localized extinction ultimately led to the emergence of two distinct species: *W. radicans* in the west and *W. unigemmata* in the east.

Vicariance-driven speciation in ferns has been well documented, especially in the context of biogeographic disjunctions between eastern Asia and eastern North America (Kuo et al., 2020; Wen et al., 2016; Wolf et al., 2001). However, intracontinental vicariance across the Northern Hemisphere is less understood, probably due to elevated extinction rates in western Eurasia (Milne and Abbott, 2002). In this sense, the *Woodwardia* disjunction represents one of the most extensive intracontinental fragmentation patterns known in the Northern Hemisphere, with sister species now separated by more than 5,000 km. Other plant disjunctions across the Palearctic may similarly reflect remnants of pre-Quaternary distributions. For instance, *Rhododendron* subsect. *Pontica* G.Don (Milne, 2004) shows a fragmented distribution spanning SW Eurasia, North America, Taiwan, and NE Asia, while being absent from mainland SE Asia. Comparable patterns are observed in several fern lineages, such as the *Adiantum reniforme* L. – *A. nelumboides* X.C.Zhang clade (Wang et al., 2015), which exhibits a fragmented distribution spanning Macaronesia, continental Africa, the Indian Ocean islands, and China. The *Stegnogramma* Blume clade (Kuo et al., 2020) and the relictual distribution of *Osmunda regalis* L. (Tsutsumi et al., 2021) provide further examples of such historical biogeographic patterns in ferns.

4.2. The role of climatic refugia following the fragmentation of the paleotropical belt

The Plio-Pleistocene fragmentation of the paleotropical-affinity lineage represented by *W. radicans* and *W. unigemmata* exemplifies the

crucial role of climatic refugia in shaping plant distributions across Eurasia. While *W. unigemmata* persisted in the relatively stable and topographically complex montane forests of East Asia—an area recognized as a major refugium for "Tertiary" flora—*W. radicans* became confined to archipelagos and refugial areas in the Western Palearctic, where paleotropical-affinity lineages faced more severe extinction pressures (Milne and Abbott, 2002; Tiffney, 1985). This asymmetry reflects the contrasting climatic and geographic contexts of each region: while East Asia maintained humid, forested environments at mid-latitudes, similar vegetation in Western Eurasia became increasingly restricted due to progressive aridification and glaciation. These changes, combined with major dispersal barriers such as the Sahara Desert and the Mediterranean Sea, further isolated western populations (Mairal et al., 2015, 2017; Milne and Abbott, 2002; Postigo-Mijarra et al., 2009; Tiffney, 1985). While most paleotropical lineages, such as laurel-leafed oaks, were lost to climatic shifts (Milne and Abbott, 2002; Barrón, 2003), some adapted (Kondraskov et al., 2015; Sanz-Arnal et al., 2022) or persisted in climatically stable refugia, particularly in the Atlantic regions of the Iberian Peninsula and peripheral areas such as the Macaronesian Islands (Fernández-Palacios et al., 2011; Kondraskov et al., 2015; Schuler et al., 2021; Suárez-Santiago et al., 2024).

Although *W. radicans* and its sister species *W. unigemmata* diverged in the Pliocene or early Pleistocene (Figs. 3, 6), the crown age of *W. radicans* itself was estimated in the Pleistocene, less than 0.7 Ma, with the Macaronesian populations from Madeira representing the earliest-diverging lineages. Long branches between sister species have previously been interpreted as evidence of extinction among intermediate populations (Antonelli and Sanmartín, 2011; Coello et al., 2024; Mairal et al., 2015), a process that may also be contributing to the low marginal probabilities observed for the ancestral range of the lineage (Fig. 6). Thus, our results are consistent with high extinction in continental *W. radicans* – *W. unigemmata* populations, alongside long-term persistence in stable microclimates. It is likely that *W. radicans* populations became extinct across much of the Western Palearctic during the Pliocene or early Pleistocene, persisting in Macaronesian refugia from which they later recolonized parts of the European mainland. Within Macaronesia, we found complex phylogenetic patterns. For example, the placement of some populations from the central Canary Islands (Tenerife, Gran Canaria) was only weakly supported, suggesting possible ancient population structure or secondary colonization events within the archipelago. Similarly, the exclusion of Azorean populations from the main dated tree reflects a technical decision related to their lower data completeness rather than any deep phylogenetic distinctiveness; when included, Azorean samples form a well-supported subclade (BS ≈ 88%) within the Canary + Western Palearctic cluster (Fig. S3). These uncertainties do not affect the biogeographic inference of a continental recolonization from Macaronesia, which remains robust across analyses. Colonization across Macaronesia may have been facilitated by the large number of palaeo-islands that existed between these archipelagos, potentially acting as stepping stones (Fernández-Palacios et al., 2011; Rijsdijk et al., 2014; Vitales et al., 2023). Additionally, abiotic and biotic factors—such as the islands' greater climatic stability, along with the clonal reproduction and mixed breeding system of *W. radicans*—likely favored both the colonization and long-term persistence of Macaronesian populations, as has been suggested for other paleotropical fern lineages (Schuler et al., 2021; Suárez-Santiago et al., 2024). In line with this, Macaronesian populations of *W. radicans* exhibit higher levels of genetic diversity than their continental counterparts, and a combination of early-diverging and later-diverging branches indicating a long-term process of lineage divergence in these archipelagos (Patiño et al., 2015; Schuler et al., 2021). Furthermore, environmental niche reconstructions are consistent with long-term persistence of *W. radicans* in Macaronesian archipelagos (including Madeira, the Azores and the Canary Islands) since at least the mid-Pleistocene (Fig. 7b), and more limited and fluctuating suitability in continental areas (Fig. 7), except for a stable suitability along the Iberian Atlantic coast.

The ancestral range reconstruction (Fig. 6) supports a west-to-east recolonization of *W. radicans* during the late Quaternary, originating in Macaronesia and expanding into various continental regions and Mediterranean islands. In our BIB analysis, posterior probabilities for ancestral ranges were generally low at deeper nodes, reflecting the high uncertainty typical of model-based biogeographic reconstructions (Ree and Smith, 2008; Matzke, 2013). Accordingly, no single ancestral area can be confidently inferred at these nodes. Nevertheless, the probability for a Macaronesian origin of the *W. radicans* crown (0.76) represents a moderately well-supported estimate within this analytical framework. Populations appear to have first recolonized Atlantic Iberia from Macaronesia, and subsequently dispersed into other parts of the Mediterranean Basin, including the Italian Peninsula, Corsica, Sicily, and Crete (Fig. 6). The role of Macaronesia as a refuge and source of relict paleotropical biodiversity has long been argued (Fernández-Palacios et al., 2011). However, alternative but compatible scenarios, such as ancient population structure followed by differential extinction or incomplete lineage sorting among refugial lineages, could also have contributed to the observed patterns.

A relictual status in Macaronesia has been suggested for other fern species such as *Adiantum reniforme* (Wang et al., 2015), *Diplazium caudatum* (Schuler et al., 2021), and *Culcita macrocarpa* (Suárez-Santiago et al., 2024). In these species, continental populations experienced genetic bottlenecks—sometimes leading to extinction, as in *D. caudatum*—during the Last Glacial Maximum, whereas island populations in the Macaronesian archipelagos persisted and retained higher genetic diversity. This pattern is well documented in *D. caudatum* (Schuler et al., 2021) and *C. macrocarpa* (Suárez-Santiago et al., 2024), and aligns with our findings in *W. radicans*. This species exhibits markedly higher genetic diversity in Macaronesian populations compared to their continental counterparts, consistent with long-term persistence, highlighting historical connectivity. These results support the hypothesis that Macaronesian islands acted as critical glacial refugia for paleotropical-affinity fern lineages, with subsequent recolonization of continental areas, primarily in the last million years. Other taxa exhibit similar island–continent dynamics—although with differences in temporal scales and inferred by different molecular markers and methods—and together provide comparative evidence for back-colonization rather than simple refugial persistence (Table 4). This recolonization was likely facilitated by the high dispersal capacity of fern spores (Wolf et al., 2001). Wind-driven dispersal from Macaronesia to the continent is a plausible mechanism, as suggested by prevailing westerly airflow patterns during Pleistocene climatic oscillations (Rognon and Coudé-Gaussen, 1996; Uriarte Cantolla, 2003), although direct evidence is not available.

These findings challenge the traditional view that continental enclaves acted as ancient pre-Quaternary, or "Tertiary," refugia for paleotropical-affinity taxa such as *W. radicans* (Pichi-Sermolli, 1979). While it remains plausible that *W. radicans* inhabited these enclaves during the Plio-Pleistocene, the genetic and biogeographic evidence suggests that such populations were subsequently lost to extinction and replaced by more recent recolonization events from Macaronesia. Nevertheless, additional lines of evidence—such as the presence of *W. radicans* along the Atlantic coast of the Iberian Peninsula throughout the late Quaternary, even before the Last Interglacial (Fig. 7c–g)—indicate that at least some continental populations may have persisted as relicts through more recent climatic fluctuations.

5. Conclusions

Our study supports the hypothesized fragmentation of an ancient belt of paleotropical flora that facilitated biotic exchange across the Northern Hemisphere. The current distribution of Woodwardioideae is consistent with a vicariance-driven speciation process shaped by historical climatic shifts. Notably, we identified intracontinental vicariance on both sides of Eurasia between *W. radicans* and *W. unigemmata* during

Table 4
Examples of organisms providing evidence of intraspecific diversity refugia in Macaronesia, with a potential subsequent recolonization of continental areas. In the third column, the crown age is provided when back-colonization age is not available.

Organism	Molecular data	Crown age / back-colonization age	Reference
Bituminaria bituminosa (L.) C. H.Stirt.	Chloroplast DNA and microsatellites	1.02 Ma (0.31–2.06)	García-Verdugo et al., 2021
Convolvulus fernandesii P.Silva & Teles	ITS	–	Carine et al., 2004
Culcita macrocarpa C.Presl	Chloroplast DNA and microsatellites	–	Suárez-Santiago et al., 2024
Diplazium caudatum (Cav.) Jermy	Microsatellites	<0.98 Ma	Schuler et al., 2021
Euphorbia balsamifera Aiton	HybSeq	0.72 Ma, 0.83 Ma	Rincón-Barrado et al., 2024
Fissidens serrulatus Brid.	Chloroplast DNA and nuclear DNA loci	Middle Pleistocene	Patiño et al., 2015
Platyhypnidium riparioides (Hedw.) Dixon	Microsatellites	Post-Glacial Maximum	Hutsemékers et al., 2011
Radula lindenbergiana Gottsche ex C. Hartm.	Chloroplast DNA	Post-Glacial Maximum	Laenen et al., 2011
Several Atlantic Bryophytes	Chloroplast DNA and nuclear DNA loci	Late Pleistocene	Patiño et al., 2015

the Pliocene-Pleistocene, where intermediate populations went extinct, leaving these species confined to the opposing ends of Eurasia, within refugial remnants of paleotropical-affinity (lauroid) forests. In the western part of the distribution, continental populations of *W. radicans* probably went extinct, retreating to Macaronesian archipelagos, from where they recolonized small European continental enclaves in the late Pleistocene. These findings underscore the role of peripheral islands as both crucial reservoirs of diversity for paleotropical-affinity relicts once widespread across the continent, as well as important sources of genetic diversity for continental enclaves. The conservation of Macaronesian refugia is therefore critical for preserving these unique lineages. Similarly, continental refugia, though more recent, hold significant conservation value as they harbor the last continental populations of ancient lineages severely threatened by climate change. The extinction debt impacting subtropical flora (Mairal et al., 2018) is likely to extend to paleotropical-affinity lineages, highlighting the urgent need for proactive conservation efforts to protect these ecosystems in the face of ongoing threats of climate change and habitat alteration. We emphasize the importance of integrating both historical and contemporary climatic dynamics into conservation strategies to effectively preserve the unique biodiversity of paleotropical-affinity lineages.

CRediT authorship contribution statement

Guillermo Santos: Data curation, Investigation, Formal analysis, Writing (original draft). **Mario Fernández-Mazuecos:** Investigation, Supervision, Formal analysis, Writing (review and editing). **Cornelia Krause:** Data curation, Investigation, Writing (review and editing). **Sonia Molino:** Data curation, Investigation, Writing (review and editing). **Anita Roth-Nebelsick:** Data curation. **Mike Thiv:** Conceptualization, Fieldwork, Funding acquisition, Investigation, Writing (review and editing). **Mario Mairal:** Conceptualization, Fieldwork, Investigation, Supervision, Formal analysis, Writing (original draft). All authors contributed to the revision of the manuscript, with Mario Mairal, Mario Fernández-Mazuecos and Guillermo Santos contributing more extensively to the review and editing stages.

Declaration of competing interest

The authors declare that they have no known competing financial interests or personal relationships that could have appeared to influence the work reported in this paper.

Acknowledgements

We thank the Real Jardín Botánico (CSIC, Madrid), the Parque Natural Fragas do Eume, authorities of the Canary Islands and the Sociedad de Ciencias Aranzadi for providing information on population locations and for their assistance during fieldwork or collection permits. We also acknowledge the help in the field from Rafael Marquina Blasco, Arnoldo Santos-Guerra (La Palma) and Paulina Kondraskov (Stuttgart), who additionally conducted preliminary lab work. We thank Ángela Aguado-Lara and Alberto Coello for their advice with some analyses. We are grateful to the Herbaria TNS, HAST and MAIC, the Tsukuba Botanical Garden (Japan), the Shanghai Chenshan Botanical Garden (China) and Cristina Blandino (University of Catania), Alfred Schäfer-Verwimp (Herdwangen-Schönach), and Nuno Oliviera (Lisboa) for providing leaf material. We also thank the two anonymous reviewers for their constructive comments, which helped improve the clarity and rigor of this manuscript. M.F.-M was supported by a Ramón y Cajal Fellowship (RYC2022- 036418-I), funded by the Spanish Ministry of Science and Innovation (MCIN/AEI/10.13039/501100011033) and the European Social Fund Plus (FSE +).

Appendix A. Supplementary data

Supplementary data to this article can be found online at https://doi.org/10.1016/j.ympev.2026.108551.

Data availability

GenBank accession numbers for three chloroplast markers are shown in Supplementary data (Table S1). Demultiplexed data were deposited in the Sequence Read Archive (NCBI) under BioProject ID PRJNA1402703

References

Aguado-Lara, Á., Sanmartín, I., Le Roux, J.J., García-Verdugo, C., Molino, S., Convey, P., Jansen van Vuuren, B., Mairal, M., 2025. Tracing the biogeographic history of the world's most isolated insular floras. J. Syst. Evol. 63 (4), 952–973. https://doi.org/10.1111/jse.13170.

Alvarez, L.W., Alvarez, W., Asaro, F., Michel, H.V., 1980. Extraterrestrial cause for the Cretaceous–Tertiary extinction. Science 208 (4448), 1095–1108. https://doi.org/10.1126/science.208.4448.109.

Antonelli, A., Sanmartín, I., 2011. Mass extinction, gradual cooling, or rapid radiation? Reconstructing the spatiotemporal evolution of the ancient angiosperm genus *Hedyosmum* (Chloranthaceae) using empirical and simulated approaches. Syst. Biol. 60 (5), 596–615. https://doi.org/10.1093/sysbio/syr062.

Axelrod, D.I., 1958. Evolution of the Madro-Tertiary geoflora. Bot. Rev. 24 (7), 433–509.

Axelrod, D.I., 1975. Evolution and biogeography of Madrean-Tethyan sclerophyll vegetation. Ann. Mo. Bot. Gard. 62 (2), 280–334. https://doi.org/10.2307/2395199.

Axelrod, D.I., Raven, P.H., 1978. Late Cretaceous and Tertiary vegetation history of Africa. In: Werger, M.J.A. (Ed.), Biogeography and Ecology of Southern Africa. Springer, Netherlands, pp. 77–130. https://doi.org/10.1007/978-94-009-9951-0_5.

Baele, G., Lemey, P., Bedford, T., Rambaut, A., Suchard, M.A., Alekseyenko, A.V., 2012. Improving the accuracy of demographic and molecular clock model comparison while accommodating phylogenetic uncertainty. Mol. Biol. Evol. 29 (9), 2157–2167. https://doi.org/10.1093/molbev/mss084.

Barrón, E., 2003. Evolución de las floras terciarias en la Península Ibérica. Monogr. Real Jard. Bot. Córdoba 11, 63–74.

Barrón, E., Rivas-Carballo, R., Postigo-Mijarra, J.M., Alcalde-Olivares, C., Vieira, M., Castro, L., Pais, J., Valle-Hernández, M., 2010. The Cenozoic vegetation of the Iberian Peninsula: A synthesis. Rev. Palaeobot. Palynol. 162 (3), 382–402. https://doi.org/10.1016/j.revpalbo.2009.11.007.

Beerling, D.J., Taylor, L.L., Bradshaw, C.D.C., Lunt, D.J., Valde, P.J., Banwart, S.A., Pagani, M., Leake, J.R., 2012. Ecosystem CO_2 starvation and terrestrial silicate weathering: Mechanisms and global-scale quantification during the late Miocene. J. Ecol. 100 (1), 31–41. https://doi.org/10.1111/j.1365-2745.2011.01905.x.

Benítez-Benítez, C., Escudero, M., Rodríguez-Sánchez, F., Martín-Bravo, S., Jiménez-Mejías, P., 2018. Pliocene–Pleistocene ecological niche evolution shapes the phylogeography of a Mediterranean plant group. Mol. Ecol. 27 (7), 1696–1713. https://doi.org/10.1111/mec.14567.

Boria, R.A., Olson, L.E., Goodman, S.M., Anderson, R.P., 2014. Spatial filtering to reduce sampling bias can improve the performance of ecological niche models. Ecol. Model. 275, 73–77. https://doi.org/10.1016/j.ecolmodel.2013.12.012.

Brown, J.L., Hill, D.J., Dolan, A.M., Carnaval, A.C., Haywood, A.M., 2018. PaleoClim, high spatial resolution paleoclimate surfaces for global land areas. Sci. Data 5, 180254. https://doi.org/10.1038/sdata.2018.254.

Calleja, J.A., Garzón, M.B., Ollero, H.S., 2009. A Quaternary perspective on the conservation prospects of the Tertiary relict tree *Prunus lusitanica* L. J. Biogeogr. 36 (3), 487–498. https://doi.org/10.1111/j.1365-2699.2008.01976.x.

Carapeto, A., Francisco, A., Pereira, P., Porto, M. (Eds.), 2020. Lista Vermelha da Flora Vascular de Portugal Continental. Imprensa Nacional, Lisboa.

Carine, M.A., Russell, S.J., Santos-Guerra, A., Francisco-Ortega, J., 2004. Relationships of the Macaronesian and Mediterranean floras: Molecular evidence for multiple colonizations into Macaronesia and back-colonization of the continent in *Convolvulus* (Convolvulaceae). Am. J. Bot. 91 (7), 1070–1085. https://doi.org/10.3732/ajb.91.7.1070.

Chaney, R.W., 1959. Miocene Floras of the Columbia Plateau. Part I. Composition and Interpretation. Carnegie Institution of Washington, Washington, DC.

Chen, T.-Y., Lou, A.-R., 2019. Phylogeography and paleodistribution models of a widespread birch (*Betula platyphylla* Suk.) across East Asia: Multiple refugia, multidirectional expansion, and heterogeneous genetic pattern. Ecol. Evol. 9 (13), 7792–7807. https://doi.org/10.1002/ece3.5365.

Coello, A.J., Vargas, P., Cano, E., Riina, R., Fernández-Mazuecos, M., 2024. Phylogenetics and phylogeography of *Euphorbia canariensis* reveal an extreme Canarian-Asian disjunction but limited inter-island colonization. Plant Biol. 26 (3), 398–414. https://doi.org/10.1111/plb.13635.

Collinson, M.E., 1992. Vegetational and floristic changes around the Eocene/Oligocene boundary in Western and Central Europe. In: Prothero, D.R., Berggren, W.A. (Eds.), Eocene–Oligocene Climatic and Biotic Evolution. Princeton University Press, Princeton, pp. 437–450.

Collinson, M.E., 2001. Cainozoic ferns and their distribution. Brittonia 53 (2), 173–235. https://doi.org/10.1007/BF02812700.

Cranfill, R., Kato, M., 2003. Phylogenetics, biogeography, and classification of the Woodwardioid ferns (Blechnaceae). In: Chandra, S., Srivastava, M. (Eds.), Pteridology in the New Millennium. Springer, Dordrecht, pp. 25–48. https://doi.org/10.1007/978-94-017-2811-9_4.

Crisp, M.D., Cook, L.G., 2007. A congruent molecular signature of vicariance across multiple plant lineages. Mol. Phylogenet. Evol. 43 (3), 1106–1117. https://doi.org/10.1016/j.ympev.2007.02.030.

Darriba, D., Taboada, G.L., Doallo, R., Posada, D., 2012. jModelTest 2: more models, new heuristics and parallel computing. Nat. Methods 9 (8), 772. https://doi.org/10.1038/nmeth.2109.

De Kort, H., Prunier, J.G., Ducatez, S., Honnay, O., Baguette, M., Stevens, V.M., Blanchet, S., 2021. Life history, climate and biogeography interactively affect worldwide genetic diversity of plant and animal populations. Nat. Commun. 12 (1), 516. https://doi.org/10.1038/s41467-021-20958-2.

Donoghue, P.C.J., Benton, M.J., 2007. Rocks and clocks: calibrating the Tree of Life using fossils and molecules. Trends Ecol. Evol. 22 (8), 424–431. https://doi.org/10.1016/j.tree.2007.05.005.

Donoghue, M.J., Bell, C.D., Li, J., 2001. Phylogenetic patterns in northern hemisphere plant geography. Int. J. Plant Sci. 162 (S6), S41–S52. https://doi.org/10.1086/323278.

Dormann, C.F., Elith, J., Bacher, S., Buchmann, C., Carl, G., Carré, G., García Marquéz, J. R., Gruber, B., Lafourcade, B., Leitão, P.J., Münkemüller, T., McClean, C., Osborne, P.E., Reineking, B., Schröder, B., Skidmore, A.K., Zurell, D., Lautenbach, S., 2013. Collinearity: a review of methods to deal with it and a simulation study evaluating their performance. Ecography 36 (1), 27–46. https://doi.org/10.1111/j.1600-0587.2012.07348.x.

Drummond, A.J., Ho, S.Y.W., Phillips, M.J., Rambaut, A., 2006. Relaxed phylogenetics and dating with confidence. PLoS Biol. 4, e88. https://doi.org/10.1371/journal.pbio.0040088.

Eaton, D.A.R., 2014. PyRAD: assembly of de novo RADseq loci for phylogenetic analyses. Bioinformatics 30 (13), 1844–1849. https://doi.org/10.1093/bioinformatics/btu121.

Eaton, D.A.R., Overcast, I., 2020. ipyrad: interactive assembly and analysis of RADseq datasets. Bioinformatics 36 (8), 2592–2594. https://doi.org/10.1093/bioinformatics/btz966.

Edgar, RC, 2004. MUSCLE: multiple sequence alignment with high accuracy and high throughput. Nucleic Acids Res. 32 (5), 1792–1797. https://doi.org/10.1093/nar/gkh340.

Elith, J., Phillips, S.J., Hastie, T., Dudík, M., Chee, Y.E., Yates, C.J., 2011. A statistical explanation of MaxEnt for ecologists. Divers. Distrib. 17 (1), 43–57. https://doi.org/10.1111/j.1472-4642.2010.00725.x.

Engler, A., 1882. Versuch einer Entwicklungsgeschichte der Pflanzenwelt, insbesondere der Florengebiete seit der Tertiärperiode. Vol 2. Die extratropischen Gebiete der Südlichen Hemisphäre und die tropischen Gebiete. W. Engelmann, Leipzig.

Fernández-Mazuecos, M., Mellers, G., Vigalondo, B., Sáez, L., Vargas, P., Glover, B.J., 2018. Resolving recent plant radiations: power and robustness of genotyping-by-sequencing. Syst. Biol. 67 (2), 250–268. https://doi.org/10.1093/sysbio/syx062.

Fernández-Palacios, J.M., de Nascimento, L., Otto, R., Delgado, J.D., García-del-Rey, E., Arévalo, J.R., Whittaker, R.J., 2011. A reconstruction of Palaeo-Macaronesia, with particular reference to the long-term biogeography of the Atlantic island laurel forests. J. Biogeogr. 38 (2), 226–246. https://doi.org/10.1111/j.1365-2699.2010.02427.x.

Freeland, J.R., Kirk, H., Petersen, S., 2011. Molecular Ecology, 2nd ed. Wiley-Blackwell, Chichester.

Freyman, W.A., Höhna, S., 2018. Cladogenetic and anagenetic models of chromosome number evolution: a Bayesian model averaging approach. Syst. Biol. 67 (2), 195–215. https://doi.org/10.1093/sysbio/syx076.

García-Verdugo, C., Mairal, M., Tamaki, I., Msanda, F., 2021. Phylogeography at the crossroad: Pleistocene range expansion throughout the Mediterranean and back-colonization from the Canary Islands in the legume *Bituminaria bituminosa*. J. Biogeogr. 48 (7), 1622–1634. https://doi.org/10.1111/jbi.14100.

Gasper, A.L., Almeida, T.E., Dittrich, V.A., de O Smith, A.R., Salino, A., 2017. Molecular phylogeny of the fern family Blechnaceae (Polypodiales) with a revised genus-level treatment. Cladistics 33 (4), 429–446. https://doi.org/10.1111/cla.12173.

Gernhard, T., 2008. The conditioned reconstructed process. J. Theor. Biol. 253 (4), 769–778. https://doi.org/10.1016/j.jtbi.2008.04.005.

Góis-Marques, C.A., Madeira, J., Menezes de Sequeira, M., 2018. Inventory and review of the Mio–Pleistocene São Jorge flora (Madeira Island, Portugal): Palaeoecological and biogeographical implications. J. Syst. Palaeontol. 16 (2), 159–177. https://doi.org/10.1080/14772019.2017.1282991.

Graham, A., 2018. The role of land bridges, ancient environments, and migrations in the assembly of the North American flora. J. Syst. Evol. 56 (5), 405–429. https://doi.org/10.1111/jse.12302.

Guerra Montes, M.J., 2018. Orígenes y Evolución de la Flora Ibérica: Estado Actual del Conocimiento. Universidad de Murcia, Murcia.

Hamon, N., Sepulchre, P., Lefebvre, V., Ramstein, G., 2013. The role of eastern Tethys seaway closure in the Middle Miocene Climatic Transition (ca. 14 Ma). Clim. Past 9 (6), 2687–2702. https://doi.org/10.5194/cp-9-2687-2013.

Heer, O., 1855-1859. Flora Tertiaria Helvetiae: The Tertiary Flora of Switzerland. Verlag der Lithographischen Anstalt von J. Wurster & Compagnie, Winterthur.

Herbert, T.D., Lawrence, K.T., Tzanova, A., Peterson, L.C., Caballero-Gill, R., Kelly, C.S., 2016. Late Miocene global cooling and the rise of modern ecosystems. Nat. Geosci. 9, 843–847. https://doi.org/10.1038/ngeo2813.

Hewitt, G.M., 1999. Post-glacial re-colonization of European biota. Biol. J. Linnean Soc. 68 (1–2), 87–112. https://doi.org/10.1111/j.1095-8312.1999.tb01160.x.

Hewitt, G.M., 2000. The genetic legacy of the Quaternary ice ages. Nature 405 (6789), 907–913. https://doi.org/10.1038/35016000.

Hewitt, G.M., 2011. Mediterranean peninsulas: The evolution of hotspots. In: Zachos, F. E., Habel, J.C. (Eds.), Biodiversity Hotspots: Distribution and Protection of Conservation Priority Areas. Springer, pp. 123–147. https://doi.org/10.1007/978-3-642-20992-5_7.

Höhna, S., Landis, M.J., Heath, T.A., Boussau, B., Lartillot, N., Moore, B.R., Huelsenbeck, J.P., Ronquist, F., 2016. RevBayes: Bayesian phylogenetic inference using graphical models and an interactive model-specification language. Syst. Biol. 65 (4), 726–736. https://doi.org/10.1093/sysbio/syw021.

Hsu, J., 1983. Late Cretaceous and Cenozoic vegetation in China, emphasizing their connections with North America. Ann. Mo. Bot. Gard. 70 (3), 490–508. https://doi.org/10.2307/2992084.

Hudson, R.R., Slatkin, M., Maddison, W.P., 1992. Estimation of levels of gene flow from DNA sequence data. Genetics 132 (2), 583–589. https://doi.org/10.1093/genetics/132.2.583.

Hutsemékers, V., Szövényi, P., Shaw, A.J., González-Mancebo, J.-M., Muñoz, J., Vanderpoorten, A., 2011. Oceanic islands are not sinks of biodiversity in spore-producing plants. Proc. Natl. Acad. Sci. U.S.A. 108 (47), 18989–18994. https://doi.org/10.1073/pnas.1109119108.

Il'inskaya, I.A., Pneva, G.P., 1984. Paporotniki oligotsenovoj flory gory Ashutas v Kazakhstane. Bot. Žurn. 69 (5), 595–604.

Karger, D.N., Conrad, O., Böhner, J., Kawohl, T., Kreft, H., Soria-Auza, R.W., Zimmermann, N.E., Linder, H.P., Kessler, M., 2017. Climatologies at high resolution for the earth's land surface areas. Sci. Data 4, 170122. https://doi.org/10.1038/sdata.2017.122.

Kearse, M., Moir, R., Wilson, A., Stones-Havas, S., Cheung, M., Sturrock, S., Buxton, S., Cooper, A., Markowitz, S., Duran, C., Thierer, T., Ashton, B., Meintjes, P., Drummond, A., 2012. Geneious Basic: an integrated and extendable desktop software platform for the organization and analysis of sequence data. Bioinformatics 28 (12), 1647–1649. https://doi.org/10.1093/bioinformatics/bts199.

Kelchner, S.A., 2000. The evolution of non-coding chloroplast DNA and its application in plant systematics. Ann. Mo. Bot. Gard. 87 (4), 482–498. https://doi.org/10.2307/2666142.

Klotz, S., Fauquette, S., Combourieu-Nebout, N., Uhl, D., Suc, J.-P., Mosbrugger, V., 2006. Seasonality intensification and long-term winter cooling as a part of the late Pliocene climate development. Earth Planet. Sci. Lett. 241 (1), 174–187. https://doi.org/10.1016/j.epsl.2005.10.005.

Kondraskov, P., Schütz, N., Schüßler, C., Sequeira, M.M., de Guerra, A.S., Caujapé-Castells, J., Jaén-Molina, R., Marrero-Rodríguez, A., Koch, M.A., Linder, P., Kovar-Eder, J., Thiv, M., 2015. Biogeography of Mediterranean hotspot biodiversity: re-evaluating the "Tertiary relict" hypothesis of Macaronesian laurel forests. PLoS One 10 (7), e0132091. https://doi.org/10.1371/journal.pone.0132091.

Kovar-Eder, J., Kvaček, Z., Martinetto, E., Roiron, P., 2006. Late Miocene to Early Pliocene vegetation of southern Europe (7–4 Ma) as reflected in the megafossil plant record. Paleogeogr. Paleoclimatol. Paleoecol. 238 (1–4), 321–339. https://doi.org/10.1016/j.palaeo.2006.03.031.

Kramer-Schadt, S., Niedballa, J., Pilgrim, J.D., Schröder, B., Lindenborn, J., Reinfelder, V., Stillfried, M., Heckmann, L., Scharf, A.K., Augeri, D.M., Cheyne, S.M., Hearn, A.J., Ross, J., Macdonald, D.W., Mathai, J., Eaton, J., Marshall, A.J., Semiadi, G., Rustam, R., Bernunga, F., Dinata, Y., Ario, A., Mardiastuti, A.,

Wilting, A., 2013. The importance of correcting for sampling bias in MaxEnt species distribution models. Divers. Distrib. 19 (11), 1366–1379. https://doi.org/10.1111/ddi.12096.
Krause, C., Oelschlägel, B., Mahfoud, H., Frank, D., Lecocq, G., Shuka, L., Neinhuis, C., Vargas, P., Tosunoglu, A., Thiv, M., Wanke, S., 2022. The evolution of the *Aristolochia pallida* complex (Aristolochiaceae) challenges traditional taxonomy and reflects large-scale glacial refugia in the Mediterranean. Ecol. Evol. 12 (4), e8765. https://doi.org/10.1002/ece3.8765.
Krijgsman, W., Hilgen, F.J., Raffi, I., Sierro, F.J., Wilson, D.S., 1999. Chronology, causes and progression of the Messinian salinity crisis. Nature 400, 652–655. https://doi.org/10.1038/23231.
Kuo, L.Y., Chang, Y.H., Huang, Y.H., Testo, W., Ebihara, A., Rouhan, G., Quintanilla, L. G., Watkins Jr., J.E., Huang, Y.M., Li, F.W., 2020. A global phylogeny of *Stegnogramma* ferns (Thelypteridaceae): generic and sectional revision, historical biogeography and evolution of leaf architecture. Cladistics 36 (2), 164–183. https://doi.org/10.1111/cla.12399.
Kvaček, Z., Teodoridis, V., Radoň, M., 2018. Review of the late Oligocene flora of Matrý near Sebuzín (České středohoří Mts., the Czech Republic). Foss. Impr. 74 (3–4), 292–316. https://doi.org/10.2478/if-2018-0018.
Laenen, B., Désamoré, A., Devos, N., Shaw, A.J., González-Mancebo, J.M., Carine, M.A., Vanderpoorten, A., 2011. Macaronesia: a source of hidden genetic diversity for post-glacial recolonization of western Europe in the leafy liverwort *Radula lindenbergiana*. J. Biogeogr. 38 (4), 631–639. https://doi.org/10.1111/j.1365-2699.2010.02440.x.
Leaché, A.D., Banbury, B.L., Felsenstein, J., Nieto-Montes de Oca, A., Stamatakis, A., 2015. Short tree, long tree, right tree, wrong tree: New acquisition bias corrections for inferring SNP phylogenies. Syst. Biol. 64 (6), 1032–1047. https://doi.org/10.1093/sysbio/syv053.
Lee, G.E., Condamine, F.L., Bechteler, J., Pérez-Escobar, O.A., Scheben, A., Schäfer-Verwimp, A., Pócs, T., Heinrichs, J., 2020. An ancient tropical origin, dispersals via land bridges and Miocene diversification explain the subcosmopolitan disjunctions of the liverwort genus *Lejeunea*. Sci. Rep. 10 (1), 14123. https://doi.org/10.1038/s41598-020-71039-1.
Löve Á, Löve D, & Pichi Sermolli REG. 1977. Cytotaxonomical Atlas of the Pteridophyta. J. Cramer, Vaduz.
Lynch, M., 2008. Estimation of nucleotide diversity, disequilibrium coefficients, and mutation rates from high-coverage genome-sequencing projects. Mol. Biol. Evol. 25 (11), 2409–2419. https://doi.org/10.1093/molbev/msn185.
Mai, D.H., 1989. Development and regional differentiation of the European vegetation during the Tertiary. Plant Syst. Evol. 162 (1–4), 79–91. https://doi.org/10.1007/BF00936911.
Mai, D.H., 1991. Palaeofloristic changes in Europe and the confirmation of the Arctotertiary-Palaeotropical geofloral concept. Rev. Palaeobot. Palynol. 68 (1), 29–36. https://doi.org/10.1016/0034-6667(91)90055-8.
Mairal, M., Pokorny, L., Aldasoro, J.J., Alarcón, M., Sanmartín, I., 2015. Ancient vicariance and climate-driven extinction explain continental-wide disjunctions in Africa: the case of the Rand Flora genus *Canarina* (Campanulaceae). Mol. Ecol. 24 (6), 1335–1354. https://doi.org/10.1111/mec.13114.
Mairal, M., Sanmartín, I., Pellissier, L., 2017. Lineage-specific climatic niche drives the tempo of vicariance in the Rand Flora. J. Biogeogr. 44 (4), 911–923. https://doi.org/10.1111/jbi.12930.
Mairal, M., Caujapé-Castells, J., Pellissier, L., Jaén-Molina, R., Álvarez, N., Heuertz, M., Sanmartín, I., 2018. A tale of two forests: Ongoing aridification drives population decline and genetic diversity loss at continental scale in Afro-Macaronesian evergreen-forest archipelago endemics. Ann. Bot. 122 (6), 1005–1017. https://doi.org/10.1093/aob/mcy107.
Maldonado, C., Molina, C.I., Zizka, A., Persson, C., Taylor, C.M., Albán, J., Chilquillo, E., Rønsted, N., Antonelli, A., 2015. Estimating species diversity and distribution in the era of Big Data: to what extent can we trust public databases? Glob. Ecol. Biogeogr. 24 (8), 973–984. https://doi.org/10.1111/geb.12326.
Mastretta-Yanes, A., Arrigo, N., Alvarez, N., Jorgensen, T.H., Piñero, D., Emerson, B.C., 2015. Restriction site-associated DNA sequencing, genotyping error estimation and *de novo* assembly optimization for population genetic inference. Mol. Ecol. Resour. 15 (1), 28–41. https://doi.org/10.1111/1755-0998.12291.
Matzke, N.J., 2013. Probabilistic historical biogeography: New models for founder-event speciation, imperfect detection, and fossils allow improved accuracy and model-testing. Front. Biogeogr. 5 (4), 242–248. https://doi.org/10.21425/F55419694.
McElwain, J.C., 2018. Paleobotany and global change: Important lessons for species to biomes from vegetation responses to past global change. Annu. Rev. Plant Biol. 69, 761–787. https://doi.org/10.1146/annurev-arplant-042817-040405.
McLaughlin, S.P., 1994. Floristic plant geography: The classification of floristic areas and floristic elements. Prog. Phys. Geogr.: Earth Environ. 18 (2), 185–208. https://doi.org/10.1177/030913339401800202.
Médail, F., Diadema, K., 2009. Glacial refugia influence plant diversity patterns in the Mediterranean Basin. J. Biogeogr. 36 (7), 1333–1345. https://doi.org/10.1111/j.1365-2699.2008.02051.x.
Migliore, J., Baumel, A., Juin, M., Médail, F., 2012. From Mediterranean shores to central Saharan mountains: Key phylogeographical insights from the genus *Myrtus*. J. Biogeogr. 39 (5), 942–956. https://doi.org/10.1111/j.1365-2699.2011.02646.x.
Milne, R.I., 2004. Phylogeny and biogeography of *Rhododendron* subsection *Pontica*, a group with a tertiary relict distribution. Mol. Phylogenet. Evol. 33 (2), 389–401. https://doi.org/10.1016/j.ympev.2004.06.009.
Milne, R.I., Abbott, R.J., 2002. The origin and evolution of Tertiary relict floras. Adv. Bot. Res. 38, 281–314. https://doi.org/10.1016/S0065-2296(02)38033-9.
Molino, S., Gabriel y Galán, J.M., Sessa, E.B., Wasowicz, P., 2019. A multi-character analysis of *Struthiopteris* leads to the rescue of *Spicantopsis* (Blechnaceae, Polypodiopsida). Taxon 68 (2), 185–198. https://doi.org/10.1002/tax.12036.
Muñoz, J., Felicísimo, A.M., Cabezas, F., Burgaz, A.R., Martínez, I., 2004. Wind as a long-distance dispersal vehicle in the Southern Hemisphere. Science 304 (5674), 1144–1147. https://doi.org/10.1126/science.1095210.
Nei, M., 1987. Molecular Evolutionary Genetics. Columbia University Press, New York, Chichester, West Sussex.
Nichols, D.J., Johnson, K.R., 2008. Plants and the K–T Boundary. Cambridge University Press, Cambridge.
Nieto Feliner, G., 2014. Patterns and processes in plant phylogeography in the Mediterranean Basin: A review. Perspect. Plant Ecol. Evol. Syst. 16 (5), 265–278. https://doi.org/10.1016/j.ppees.2014.07.002.
Nogué, S., de Nascimento, L., Froyd, C.A., Wilmshurst, J.M., de Boer, E.J., Coffey, E.E.D., Whittaker, R.J., Fernández-Palacios, J.M., Willis, K.J., 2017. Island biodiversity conservation needs palaeoecology. Nat. Ecol. Evol. 1, 0181. https://doi.org/10.1038/s41559-017-0181.
Otto-Bliesner, B.L., Marshall, S.J., Overpeck, J.T., Miller, G.H., Hu, A., CAPE Last Interglacial Project members, 2006. Simulating arctic climate warmth and icefield retreat in the last interglaciation. Science 311 (5768), 1751–1753. https://doi.org/10.1126/science.1120808.
Palamarev, E., Bozukov, V., Uzunova, K., Petkova, A., Kitanov, G., 2005. Catalogue of the Cenozoic plants of Bulgaria (Eocene to Pliocene). Phytol. Balcan. 11 (3), 215–364.
Parham, J.F., Donoghue, P.C.J., Bell, C.J., Calway, T.D., Head, J.J., Holroyd, P.A., Inoue, J.G., Irmis, R.B., Joyce, W.G., Ksepka, D.T., Patané, J.S.L., Smith, N.D., Tarver, J.E., van Tuinen, M., Yang, Z., Angielczyk, K.D., Greenwood, J.M., Hipsley, C.A., Jacobs, L., Makovicky, P.J., Müller, J., Smith, K.T., Theodor, J.M., Warnock, R.C.M., Benton, M.J., 2012. Best practices for justifying fossil calibrations. Syst. Biol. 61 (2), 346–359. https://doi.org/10.1093/sysbio/syr107.
Patiño, J., Carine, M., Mardulyn, P., Devos, N., Mateo, R.G., González-Mancebo, J.M., Shaw, A.J., Vanderpoorten, A., 2015. Approximate Bayesian computation reveals the crucial role of oceanic islands for the assembly of continental biodiversity. Syst. Biol. 64 (4), 579–589. https://doi.org/10.1093/sysbio/syv013.
Pattengale, N.D., Alipour, M., Bininda-Emonds, O.R.P., Moret, B.M.E., Stamatakis, A., 2010. How many bootstrap replicates are necessary? J. Comput. Biol. 17 (3), 337–354. https://doi.org/10.1089/cmb.2009.0179.
Pelosi, J.A., Sessa, E.B., 2021. From genomes to populations: a meta-analysis and review of fern population genetics. Int. J. Plant Sci. 182 (5), 325–343. https://doi.org/10.1086/713442.
Phillips, S.J., Anderson, R.P., Schapire, R.E., 2006. Maximum entropy modeling of species geographic distributions. Ecol. Model. 190 (3-4), 231–259. https://doi.org/10.1016/j.ecolmodel.2005.03.026.
Pichi-Sermolli, R.E.G., 1979. A survey of the pteridological flora of the Mediterranean region. Webbia 34 (1), 175–242. https://doi.org/10.1080/00837792.1979.10670169.
Pigg, K.B., Devore, M.L., Wehr, W.C., 2006. Filicalean ferns from the Tertiary of Western North America: *Osmunda* L. (Osmundaceae: Pteridophyta), *Woodwardia* Sm. (Blechnaceae: Pteridophyta) and onocleoid forms (filicales: Pteridophyta). Fern Gaz. 17 (5), 279–286.
Poland, J.A., Brown, P.J., Sorrells, M.E., Jannink, J.-L., 2012. Development of high-density genetic maps for barley and wheat using a novel two-enzyme genotyping-by-sequencing approach. PLoS One 7 (2), e32253. https://doi.org/10.1371/journal.pone.0032253.
Postigo-Mijarra, J.M., Barrón, E., Gómez Manzaneque, F., Morla, C., 2009. Floristic changes in the Iberian Peninsula and Balearic Islands (south-west Europe) during the Cenozoic. J. Biogeogr. 36 (11), 2025–2043. https://doi.org/10.1111/j.1365-2699.2009.02142.x.
PPG I, 2016. A community-derived classification for extant lycophytes and ferns. J. Syst. Evol. 54 (6), 563–603. https://doi.org/10.1111/jse.12229.
QGIS Development Team, 2020. QGIS Geographic Information System. QGIS Association. https://www.qgis.org (accessed 15 January 2026).
Quintanilla, L.G., Pajarón, S., Pangua, E., Amigo, J., 2000. Effect of temperature on germination in northernmost populations of *Culcita macrocarpa* and *Woodwardia radicans*. Plant Biol. 2 (6), 612–617. https://doi.org/10.1055/s-2000-16638.
Quintanilla, L.G., Pajarón, S., Pangua, E., Amigo, J., 2007. Allozyme variation in the sympatric ferns *Culcita macrocarpa* and *Woodwardia radicans* at the northern extreme of their ranges. Plant Syst. Evol. 263 (3), 135–144. https://doi.org/10.1007/s00606-006-0486-x.
Rambaut, A., 2018. FigTree v1.4.4. Institute of Evolutionary Biology, University of Edinburgh, Edinburgh. https://github.com/rambaut/figtree (accessed 15 January 2026).
Rambaut, A., Drummond, A.J., 2018. TreeAnnotator v1.10.4: MCMC Output analysis. Institute of Evolutionary Biology, University of Edinburgh, Edinburgh. http://beast.community/treeannotator (accessed 15 January 2026).
Rambaut, A., Drummond, A.J., Xie, D., Baele, G., Suchard, M.A., 2018. Posterior summarisation in Bayesian phylogenetics using Tracer 1.7. Syst. Biol. 67 (5), 901–904. https://doi.org/10.1093/sysbio/syy032.
Rancilhac, L., Sylvestre, F., Hutter, C.R., Arntzen, J.W., Babik, W., Crochet, P.-A., Deso, G., Duguet, R., Galan, P., Pabijan, M., Policain, M., Priol, P., Sabino-Pinto, J., Capstick, M., Elmer, K.R., Dufresnes, C., Vences, M., 2023. Exploring the impact of read clustering thresholds on RADseq-based systematics: an empirical example from European amphibians. bioRxiv, 2023.04.19.537466. https://doi.org/10.1101/2023.04.19.537466.
Raymo, M.E., Ruddiman, W.F., Froelich, P.N., 1988. Influence of late Cenozoic mountain building on ocean geochemical cycles. Geology 16 (7), 649–653. https://doi.org/10.1130/0091-7613(1988)016<0649:IOLCMB>2.3.CO;2.
Ree, R.H., Smith, S.A., 2008. Maximum likelihood inference of geographic range evolution by dispersal, local extinction, and cladogenesis. Syst. Biol. 57 (1), 4–14. https://doi.org/10.1080/10635150701883881.

Renner, S.S., 2005. Relaxed molecular clocks for dating historical plant dispersal events. Trends Plant Sci. 10 (11), 550–558. https://doi.org/10.1016/j.tplants.2005.09.010.
Rijsdijk, K.F., Hengl, T., Norder, S.J., Otto, R., Emerson, B.C., Ávila, S.P., López, H., van Loon, E.E., Tjørve, E., Fernández-Palacios, J.M., 2014. Quantifying surface-area changes of volcanic islands driven by Pleistocene sea-level cycles: Biogeographical implications for the Macaronesian archipelagos. J. Biogeogr. 41 (7), 1242–1254. https://doi.org/10.1111/jbi.12336.
Rincón-Barrado, M., Villaverde, T., Perez, M.F., Sanmartín, I., Riina, R., 2024. The sweet tabaiba or there and back again: Phylogeographical history of the Macaronesian *Euphorbia balsamifera*. Ann. Bot. 133 (5–6), 883–904. https://doi.org/10.1093/aob/mcae001.
Rognes, T., Flouri, T., Nichols, B., Quince, C., Mahé, F., 2016. VSEARCH: a versatile open-source tool for metagenomics. PeerJ 4, e2584. https://doi.org/10.7717/peerj.2584.
Rognon, P., Coudé-Gaussen, G., 1996. Paleoclimates off Northwest Africa (28°–35°N) about 18,000 yr B.P. based on continental Eolian deposits. Quat. Res. 46 (2), 118–126. https://doi.org/10.1006/qres.1996.0052.
Ronquist, F., Teslenko, M., van der Mark, P., Ayres, D.L., Darling, A., Höhna, S., Larget, B., Liu, L., Suchard, M.A., Huelsenbeck, J.P., 2012. MrBayes 3.2: efficient Bayesian phylogenetic inference and model choice across a large model space. Syst. Biol. 61 (3), 539–542. https://doi.org/10.1093/sysbio/sys029.
Rozas, J., Ferrer-Mata, A., Sánchez-DelBarrio, J.C., Guirao-Rico, S., Librado, P., Ramos-Onsins, S.E., Sánchez-Gracia, A., 2017. DnaSP 6: DNA sequence polymorphism analysis of large data sets. Mol. Biol. Evol. 34 (12), 3299–3302. https://doi.org/10.1093/molbev/msx248.
Salvo Tierra, E., 1990. Guía de Helechos de la Península Ibérica y Baleares. Ediciones Pirámide, Madrid.
Sanmartín, I., Enghoff, H., Ronquist, F., 2001. Patterns of animal dispersal, vicariance and diversification in the Holarctic. Biol. J. Linn. Soc. 73 (4), 345–390. https://doi.org/10.1006/bijl.2001.0542.
Sanmartín, I., Van Der Mark, P., Ronquist, F., 2008. Inferring dispersal: a Bayesian approach to phylogeny-based island biogeography, with special reference to the Canary Islands. J. Biogeogr. 35 (3), 428–449. https://doi.org/10.1111/j.1365-2699.2007.01820.x.
Sanz-Arnal, M., Benítez-Benítez, C., Miguez, M., Jiménez-Mejías, P., Martín-Bravo, S., 2022. Are Cenozoic relict species also climatic relicts? Insights from the macroecological evolution of the giant sedges of *Carex* sect. *Rhynchocystis* (Cyperaceae). Am. J. Bot. 109 (1), 115–129. https://doi.org/10.1002/ajb2.1788.
Saporta, G.D., Marion, A.-F., Falsan, A., 1872. Recherches sur les Végétaux Fossiles de Meximieux, Précédées d'une Introduction Stratigraphique. Arch. Mus. Hist. Nat. Lyon 131–335.
Schmitt, T., 2007. Molecular biogeography of Europe: Pleistocene cycles and postglacial trends. Front. Zool. 4, 11. https://doi.org/10.1186/1742-9994-4-11.
Schuler, S.B.-M., Picazo-Aragonés, J., Rumsey, F.J., Romero-García, A.T., Suárez-Santiago, V.N., 2021. Macaronesia acts as a museum of genetic diversity of relict ferns: the case of *Diplazium caudatum* (Athyriaceae). Plants 10 (11), 2425. https://doi.org/10.3390/plants10112425.
Shafer, A.B.A., Wolf, J.B.W., Alves, P.C., Bergström, L., Bruford, M.W., Brännström, I., et al., 2015. Genomics and the challenging translation into conservation practice. Trends Ecol. Evol. 30 (2), 78–87. https://doi.org/10.1016/j.tree.2014.11.009.
Sigel, E.M., Windham, M.D., Haufler, C.H., Pryer, K.M., 2014. Phylogeny, divergence time estimates, and phylogeography of the diploid species of the *Polypodium vulgare* complex (Polypodiaceae). Syst. Bot. 39 (4), 1042–1055. https://doi.org/10.1600/036364414X683921.
Small, R.L., Lickey, E.B., Shaw, J., Hauk, W.D., 2005. Amplification of noncoding chloroplast DNA for phylogenetic studies in lycophytes and monilophytes with a comparative example of relative phylogenetic utility from Ophioglossaceae. Mol. Phylogenet. Evol. 36 (3), 509–522. https://doi.org/10.1016/j.ympev.2005.04.018.
Smith, S.A., Donoghue, M.J., 2010. Combining historical biogeography with niche modeling in the *Caprifolium* clade of *Lonicera* (Caprifoliaceae, Dipsacales). Syst. Biol. 59 (3), 322–341. https://doi.org/10.1093/sysbio/syq011.
Smith, S.A., O'Meara, B.C., 2012. treePL: divergence time estimation using penalized likelihood for large phylogenies. Bioinformatics 28 (20), 2689–2690. https://doi.org/10.1093/bioinformatics/bts492.
Stamatakis, A., 2006. RAxML-VI-HPC: Maximum likelihood-based phylogenetic analyses with thousands of taxa and mixed models. Bioinformatics 22 (21), 2688–2690. https://doi.org/10.1093/bioinformatics/btl446.
Stamatakis, A., 2014. RAxML version 8: a tool for phylogenetic analysis and post-analysis of large phylogenies. Bioinformatics 30 (9), 1312–1313. https://doi.org/10.1093/bioinformatics/btu033.
Stewart, J.R., Lister, A.M., Barnes, I., Dalén, L., 2010. Refugia revisited: individualistic responses of species in space and time. Proc. R. Soc. B 277 (1682), 661–671. https://doi.org/10.1098/rspb.2009.1272.
Suárez-Santiago, V.N., Provan, J., Romero-García, A.T., Ben-Menni, S.S., 2024. Genetic diversity and phylogeography of the relict tree fern *Culcita macrocarpa*: Influence of clonality and breeding system on genetic variation. Plants 13 (12), 12. https://doi.org/10.3390/plants13121587.
Suchard, M.A., Lemey, P., Baele, G., Ayres, D.L., Drummond, A.J., Rambaut, A., 2018. Bayesian phylogenetic and phylodynamic data integration using BEAST 1.10. Virus Evol. 4, vey016. https://doi.org/10.1093/ve/vey016.
Takahashi, T., Nagata, N., Sota, T., 2014. Application of RAD-based phylogenetics to complex relationships among variously related taxa in a species flock. Mol. Phylogenet. Evol. 80, 137–144. https://doi.org/10.1016/j.ympev.2014.07.016.
Testo, W.L., de Gasper, A.L., Molino, S., Gabriel y Galán, J.M., Salino, A., Dittrich, V.A. de.O., Sessa, E.B., 2022. Deep vicariance and frequent transoceanic dispersal shape the evolutionary history of a globally distributed fern family. Am. J. Bot. 109 (10), 1579–1595. https://doi.org/10.1002/ajb2.16062.
Thiers, B., 2025. Index Herbariorum: A Global Directory of Public Herbaria and Associated Staff. New York Botanical Garden's Virtual Herbarium, New York. http://sweetgum.nybg.org/ih/ (accessed 13 February 2025).
Tiffney, B.H., 1985. The Eocene North Atlantic land bridge: its importance in Tertiary and modern phytogeography of the Northern Hemisphere. J. Arnold Arbor. 66 (2), 243–273. https://doi.org/10.5962/bhl.part.13183.
Tiffney, B.H., Manchester, S.R., 2001. The use of geological and paleontological evidence in evaluating plant phylogeographic hypotheses in the Northern Hemisphere Tertiary. Int. J. Plant Sci. 162 (S6), S3–S17. https://doi.org/10.1086/323880.
Tonini, J., Moore, A., Stern, D., Shcheglovitova, M., Ortí, G., 2015. Concatenation and species tree methods exhibit statistically indistinguishable accuracy under a range of simulated conditions. PLoS Curr. Tree of Life. https://doi.org/10.1371/currents.tol.34260cc27551a527b124ec5f6334b6be.
Torfstein, A., Steinberg, J., 2020. The Oligo–Miocene closure of the Tethys Ocean and evolution of the proto-Mediterranean Sea. Sci. Rep. 10, 13817. https://doi.org/10.1038/s41598-020-70652-4.
Tribble, C.M., Freyman, W.A., Landis, M.J., Lim, J.Y., Barido-Sottani, J., Kopperud, B.T., Höhna, S., May, M.R., 2022. RevGadgets: an R package for visualizing Bayesian phylogenetic analyses from RevBayes. Methods Ecol. Evol. 13 (2), 314–323. https://doi.org/10.1111/2041-210X.13743.
Truszkowski, J., Perrigo, A., Broman, D., Ronquist, F., Antonelli, A., 2023. Online tree expansion could help solve the problem of scalability in Bayesian phylogenetics. Syst. Biol. 72 (5), 1199–1206. https://doi.org/10.1093/sysbio/syad045.
Tsutsumi, C., Yatabe-Kakugawa, Y., Hirayama, Y., Chiou, W.-L., Kato, M., 2021. Molecular analyses of the disjunctly distributed *Osmunda regalis* and *O. japonica* (Osmundaceae), with particular reference to introgression and hybridization. Plant Syst. Evol. 307 (3), 35. https://doi.org/10.1007/s00606-021-01751-6.
Uriarte Cantolla, A., 2003. Historia del Clima de la Tierra. Servicio Central de Publicaciones, Gobierno Vasco, Vitoria-Gasteiz.
Valcárcel, V., Guzmán, B., Medina, N.G., Vargas, P., Wen, J., 2017. Phylogenetic and paleobotanical evidence for late Miocene diversification of the Tertiary subtropical lineage of ivies (*Hedera* L., Araliaceae). BMC Evol. Biol. 17, 146. https://doi.org/10.1186/s12862-017-0984-1.
Vanderpoorten, A., Rumsey, F.J., Carine, M.A., 2007. Does Macaronesia exist? Conflicting signal in the bryophyte and pteridophyte floras. Am. J. Bot. 94 (4), 625–639. https://doi.org/10.3732/ajb.94.4.625.
Varela, S., Lobo, J.M., Hortal, J., 2011. Using species distribution models in paleobiogeography: a matter of data, predictors and concepts. Palaeogeogr. Palaeoclimatol. Palaeoecol. 310 (3–4), 451–463. https://doi.org/10.1016/j.palaeo.2011.07.021.
Villanueva Raisman, A., Sánchez de Dios, R., Domínguez Lozano, F., Villa-Machío, I., Pías, B., Sáez, L., Fernández-Mazuecos, M., Mairal, M., 2025. Population genomics and taxonomy solve a conservation conundrum in the Balearic paleoendemic *Femeniasia balearica*. Perspect. Plant Ecol. Evol. Syst. 68, 125888. https://doi.org/10.1016/j.ppees.2025.125888.
Vitales, D., Guerrero, C., Garnatje, T., Romeiras, M.M., Santos, A., Fernandes, F., Vallès, J., 2023. Parallel anagenetic patterns in endemic *Artemisia* species from three Macaronesian archipelagos. AoB Plants 15 (4), plad057. https://doi.org/10.1093/aobpla/plad057.
Vitelli, M., Vessella, F., Cardoni, S., Pollegioni, P., Denk, T., Grimm, G.W., Simeone, M.C., 2017. Phylogeographic structuring of plastome diversity in Mediterranean oaks (*Quercus* Group Ilex, Fagaceae). Tree Genet. Genomes 13, 3. https://doi.org/10.1007/s11295-016-1086-8.
Walther, H., 1994. Invasion of Arcto-Tertiary elements in the Palaeogene of Central Europe. In: Boulter, M.C., Fisher, H.C. (Eds.), Cenozoic Plants and Climates of the Arctic. Springer Berlin, Heidelberg, pp. 239–250.
Wang, A.-H., Sun, Y., Schneider, H., Zhai, J.-W., Liu, D.-M., Zhou, J.-S., Xing, F.-W., Chen, H.-F., Wang, F.-G., 2015. Identification of the relationship between Chinese *Adiantum reniforme* var. *sinense* and Canary *Adiantum reniforme*. BMC Plant Biol. 15 (1), 36. https://doi.org/10.1186/s12870-014-0361-9.
Waterhouse, A.M., Procter, J.B., Martin, D.M.A., Clamp, M., Barton, G.J., 2009. Jalview Version 2—A multiple sequence alignment editor and analysis workbench. Bioinformatics 25 (9), 1189–1191. https://doi.org/10.1093/bioinformatics/btp033.
Wen, J., Nie, Z.-L., Ickert-Bond, S.M., 2016. Intercontinental disjunctions between eastern Asia and western North America in vascular plants highlight the biogeographic importance of the Bering land bridge from late cretaceous to Neogene. J. Syst. Evol. 54 (5), 469–490. https://doi.org/10.1111/jse.12222.
Wickham, H., 2016. ggplot2: Elegant Graphics for Data Analysis. Springer-Verlag, New York.
Wolfe, J.A., 1981. A chronologic framework for Cenozoic megafossil floras of northwestern North America and its relation to marine geochronology. In: Armentrout, J.M. (Ed.), Pacific Northwest Cenozoic Biostratigraphy. Geological Society of America, Boulder, CO, pp. 39–48.
Wolfe, J.A., 1992. Climatic, floristic and vegetational changes near the Eocene/Oligocene boundary in North America. In: Prothero, D.R., Berggren, W.A. (Eds.), Eocene–Oligocene Climatic and Biotic Evolution. Princeton University Press, Princeton, pp. 421–436.
Wolfe, K.H., Li, W.H., Sharp, P.M., 1987. Rates of nucleotide substitution vary greatly among plant mitochondrial, chloroplast, and nuclear DNAs. Proc. Natl. Acad. Sci. U. S.A. 84 (24), 9054–9058. https://doi.org/10.1073/pnas.84.24.9054.
Wolf, P.G., Schneider, H., Ranker, T.A., 2001. Geographic distributions of homosporous ferns: does dispersal obscure evidence of vicariance? J. Biogeogr. 28 (2), 263–270. https://doi.org/10.1046/j.1365-2699.2001.00531.x.

Wright, K., 2018. *corrgram*: Plot a correlogram, R package version 1.13. https://CRAN.R-project.org/package=corrgram (accessed 15 January 2026).
Xiang, J.-Y., Wen, J., Peng, H., 2015. Evolution of the eastern Asian–North American biogeographic disjunctions in ferns and lycophytes. J. Syst. Evol. 53 (1), 2–32. https://doi.org/10.1111/jse.12141.
Xi, Z., Liu, L., Davis, C.C., 2016. The impact of missing data on species tree estimation. Mol. Biol. Evol. 33 (3), 838–860. https://doi.org/10.1093/molbev/msv266.
Yesson, C., Culham, A., 2006. Phyloclimatic modeling: Combining phylogenetics and bioclimatic modeling. Syst. Biol. 55 (5), 785–802. https://doi.org/10.1080/1063515060081570.
Zachos, J.C., Dickens, G.R., Zeebe, R.E., 2008. An early Cenozoic perspective on greenhouse warming and carbon-cycle dynamics. Nature 451 (7176), 279–283. https://doi.org/10.1038/nature06588.
Zizka, A., Silvestro, D., Andermann, T., Azevedo, J., Duarte Ritter, C., Edler, D., Farooq, H., Herdean, A., Ariza, M., Scharn, R., Svantesson, S., Wengström, N., Zizka, V., Antonelli, A., 2019. CoordinateCleaner: Standardized cleaning of occurrence records from biological collection databases. Methods Ecol. Evol. 10 (5), 744–751. https://doi.org/10.1111/2041-210X.13152.